

Understanding Cross-Domain Few-Shot Learning: An Experimental Study

Jaehoon Oh^{*1} Sungnyun Kim^{*2} Namgyu Ho^{*2} Jin-Hwa Kim³ Hwanjun Song³ Se-Young Yun²

Abstract

Cross-domain few-shot learning has drawn increasing attention for handling large differences between the source and target domains—an important concern in real-world scenarios. To overcome these large differences, recent works have considered exploiting small-scale unlabeled data from the target domain during the pre-training stage. This data enables self-supervised pre-training on the target domain, in addition to supervised pre-training on the source domain. In this paper, we empirically investigate scenarios under which it is advantageous to use each pre-training scheme, based on *domain similarity* and *few-shot difficulty*: performance gain of self-supervised pre-training over supervised pre-training increases when domain similarity is smaller or few-shot difficulty is lower. We further design two pre-training schemes, mixed-supervised and two-stage learning, that improve performance. In this light, we present seven findings for CD-FSL which are supported by extensive experiments and analyses on three source and eight target benchmark datasets with varying levels of domain similarity and few-shot difficulty. Our code is available at <https://anonymous.4open.science/r/understandingCDFSL>.

1. Introduction

Few-shot learning (FSL) is a machine learning paradigm to learn novel classes from *few* examples with supervised information (Vinyals et al., 2016; Wang et al., 2020). Unlike standard supervised learning, a model is pre-trained on the source dataset consisting of *base* classes and then transferred into the target dataset consisting of *novel* classes with few examples, where base and novel classes

^{*}Equal contribution ¹Graduate School of Knowledge Service Engineering, KAIST, Daejeon, South Korea ²Kim Jaechul Graduate School of Artificial Intelligence, KAIST, Seoul, South Korea ³Naver AI Lab, Seongnam, South Korea. Correspondence to: Se-Young Yun <yunseyoung@kaist.ac.kr>, Hwanjun Song <hwanjun.song@navercorp.com>.

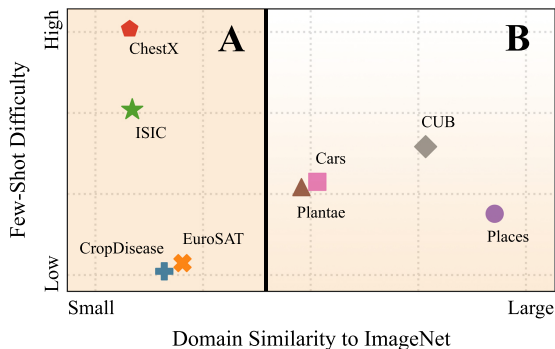


Figure 1. Our insights on the pre-training approaches. (A) SSL is preferred for all datasets with small domain similarity. (B) SSL is preferred for low-difficulty datasets with large domain similarity.

are disjoint but share similar data domains. However, this underlying assumption is not applicable to real-world scenarios because source (base classes) and target (novel classes) domains are different in general. This leads to poor generalization performance because of the change in feature and label distributions, posing a new challenge in FSL (Guo et al., 2020; Tseng et al., 2020).

In this regard, *cross-domain few-shot learning* (CD-FSL) is gaining immense attention with the BSCD-FSL (Broader Study of CD-FSL) benchmark (Guo et al., 2020), which enables us to evaluate real-world few-shot learning tasks. The BSCD-FSL benchmark is a collection of four different datasets with varying levels of domain similarity to large-scale natural image collections, such as ImageNet (Deng et al., 2009). Although there are two possible directions for FSL, meta-learning (Finn et al., 2017; Lee et al., 2019; Tseng et al., 2020) and transfer learning (Chen et al., 2019; Dhillon et al., 2020; Tian et al., 2020b), transfer learning has been reported to have higher performance than meta-learning approaches in cross-domain scenarios. Therefore, following the transfer learning pipeline, recent studies for CD-FSL have mainly focused on improving the pre-training phase before fine-tuning on the target labeled data with novel classes.

To address the challenge of different domains, there have been recent efforts to leverage *unlabeled* examples from the target domain as auxiliary data for pre-training, in addition to labeled examples from the source domain. For example, along with the supervised cross-entropy loss, STARTUP

(Phoo & Hariharan, 2021) and Dynamic Distillation (Islam et al., 2021a) incorporate distillation loss and FixMatch-like loss for self-supervision, respectively. In other words, they develop sophisticated pre-training approaches that can leverage source and target data together. However, their basic pre-training schemes, supervised learning (SL) on the source domain and self-supervised learning (SSL) on the target domain, have not been thoroughly studied with respect to their pros and cons in CD-FSL.

In this paper, we establish an empirical understanding of the effectiveness of SL and SSL for a better pre-training process in CD-FSL. To this end, we begin by scrutinizing the opposing finding of the previous works (Phoo & Hariharan, 2021; Islam et al., 2021a). We discover that readily available SSL methods, *e.g.*, SimCLR (Chen et al., 2020a), outperform the standard SL method for pre-training, even when the amount of unlabeled target data for SSL is much smaller than that of labeled source data for SL (see Section 4).

Next, we investigate how the two properties of *domain similarity* and *few-shot difficulty* affect the pre-training phase using SL and SSL. **Domain Similarity** is the similarity between the source and target domains, which is known to affect the transferability of the source domain features into the target domain. However, we find it insufficient to identify the effectiveness of SL and SSL on the basis of domain similarity alone. To solve this conundrum, we propose **Few-Shot Difficulty** as a measure of the inherent hardness of a dataset, using the upper bound of empirical FSL performance. Figure 1 describes our insights on the pre-training approaches, based on the two estimated metrics which are formally explained in Section 3.2. By incorporating few-shot difficulty into the analysis, we conclude that SSL is preferred (A) when domain similarity is small, or (B) few-shot difficulty is low under large domain similarity (see Section 5).

Finally, to investigate whether SL and SSL can synergize, we design a joint learning scheme using both SL and SSL, coined as *mixed-supervised learning* (MSL). It is observed that synergy occurs when both conditions are extreme, *i.e.*, under small domain similarity with high few-shot difficulty or large domain similarity with low few-shot difficulty. Furthermore, we extend our analysis to a *two-stage* pre-training scheme, which is motivated by the recent works for CD-FSL (Phoo & Hariharan, 2021; Islam et al., 2021a). Two-stage pre-training generally improves few-shot performance and this observation becomes clearer when domain similarity is large (see Section 6).

2. Related Work

2.1. Few-Shot Learning (FSL)

FSL has been mainly studied in the literature based on two approaches, meta-learning and transfer learning. In the meta-learning approach, a model is trained on the meta-train set

(*i.e.*, source data) in an episodic manner, mimicking the evaluation procedure, such that fast adaptation is possible on the meta-test set (*i.e.*, few-shot target data). This family of approaches include learning a good initialization (Maclaurin et al., 2015; Finn et al., 2017; 2018; Raghu et al., 2019; Oh et al., 2021), learning a metric space (Vinyals et al., 2016; Snell et al., 2017; Sung et al., 2018), and learning an update rule (Ravi & Larochelle, 2016; Andrychowicz et al., 2016; Flennerhag et al., 2020). By contrast, in the transfer-based approach (Chen et al., 2019; Dhillon et al., 2020; Tian et al., 2020b), a model is pre-trained on the source dataset following the general supervised learning procedure in a mini-batch manner, and subsequently fine-tuned on the target dataset for evaluation.

2.2. Cross-Domain Few-Shot Learning (CD-FSL)

CD-FSL has addressed a more challenging and realistic scenario where source and target domains are dissimilar (Guo et al., 2020; Tseng et al., 2020). Such a cross-domain setting makes it difficult to transfer source information into the target domain owing to large domain differences (Pan & Yang, 2009; Li et al., 2020; Neyshabur et al., 2020; Zhang et al., 2020). In general, the most recent methods have been developed on top of the fine-tuning paradigm because this paradigm outperforms the traditional meta-learning approach such as FWT (Guo et al., 2020). STARTUP (Phoo & Hariharan, 2021) and Dynamic Distillation (Islam et al., 2021a) are the two representative algorithms, and they suggested using a small unlabeled data from the target domain in pre-training such that a pre-trained model can be well-adaptable for the target domain. Specifically, both algorithms first train a teacher network with cross-entropy loss on labeled source data. Then, STARTUP trains the student network with cross-entropy loss on the source data together with two unsupervised losses on the target data: distillation loss (Hinton et al., 2015) and self-supervised loss (*i.e.*, SimCLR (Chen et al., 2020a)). Dynamic Distillation trains the student network with cross-entropy loss on labeled source data and KL loss based on FixMatch (Sohn et al., 2020) on unlabeled target data.

2.3. Self-Supervised Learning (SSL)

SSL has attracted attention as a method of learning useful representations from unlabeled data (Dosovitskiy et al., 2015; Doersch et al., 2015; Zhang et al., 2016; Pathak et al., 2016; Noroozi et al., 2017). When this field first emerged, hand-crafted pretext tasks, such as solving jigsaw puzzles (Noroozi & Favaro, 2016) and predicting rotations (Gidaris et al., 2018), were designed and utilized for training. In recent times, there has been an effort to use contrastive loss, which enhances representation learning based on the augmentation and negative samples (Chen et al., 2020a; Tian et al., 2020a; He et al., 2020; Caron et al., 2020). This contrastive loss encourages the alignment of

Table 1. Summary of the notations.

Notation	Description
$\mathcal{D}_B, \mathcal{D}_N$	Source and target datasets, $\mathcal{D}_B \cap \mathcal{D}_N = \emptyset$
$\mathcal{C}_B, \mathcal{C}_N$	Base classes for \mathcal{D}_B and novel classes for \mathcal{D}_N
$\mathcal{D}_U (\subset \mathcal{D}_N)$	Unlabeled target data for SSL
$\mathcal{D}_L (\subset \mathcal{D}_N)$	Labeled target data for evaluation, $\mathcal{D}_U \cap \mathcal{D}_L = \emptyset$
n, k	# classes and examples for n -way k -shot
$\mathcal{D}_S (\subset \mathcal{D}_L)$	A support set with size nk for fine-tuning
$\mathcal{D}_Q (\subset \mathcal{D}_L)$	A query set for evaluation, $\mathcal{D}_S \cap \mathcal{D}_Q = \emptyset$
f	A feature extractor (backbone network)
h_{sl}	A classification head for SL during pre-training
h_{ssl}	A projection head for SSL during pre-training
g	A classification head during fine-tuning

positive pairs and uniformity of data distribution on the hypersphere (Wang & Isola, 2020). This improves the transferability of a model by containing lower-level semantics compared to supervised approaches (Islam et al., 2021b). However, this advantage is conditional on the availability of numerous negative samples. To alleviate such constraints, non-contrastive approaches that do not use negative samples have been proposed (Grill et al., 2020; Chen & He, 2021). In our empirical study, we use two contrastive approaches, SimCLR (Chen et al., 2020a) and MoCo (He et al., 2020) and two non-contrastive approaches, BYOL (Grill et al., 2020) and SimSiam (Chen & He, 2021). The details of each algorithm are described in Appendix A.

For the completeness of our survey, we include prior works that address SSL for cross-domain and/or few-shot learning. Kim et al. (2021) addressed self-supervised pre-training under label-shared cross-domain, while our setting does not share the label space between domains. Ericsson et al. (2021) observed that SSL on the source data improves performance on BSCD-FSL dataset. However, domain-specific SSL (*i.e.*, SSL on target data) was not addressed. Cole et al. (2021) showed that adding data from different domains can lead to performance degradation when data is numerous. Phoo & Hariharan (2021) and Islam et al. (2021a) argued that plain SSL methods struggle to outperform SL for CD-FSL. We investigate domain-specific SSL and demonstrate its superiority, which is the opposite finding to that of previous studies.

3. Overview

In this section, we clarify the scope of our empirical study, propose formal definitions of domain similarity and few-shot difficulty, and describe experimental configurations. Table 1 summarizes the notations used in this paper.

3.1. Scope of the Empirical Study

Our objective is to learn a feature extractor f on base classes \mathcal{C}_B in source data \mathcal{D}_B , which can extract informative representations for novel classes \mathcal{C}_N in target data \mathcal{D}_N . Typically,

a classifier g is fine-tuned and the model $g \circ f$ is evaluated using labeled target examples $\mathcal{D}_L (\subset \mathcal{D}_N)$ after pre-training f on the source data \mathcal{D}_B under the condition that the base classes are largely different from the novel classes.

Following the recent literature (Phoo & Hariharan, 2021; Islam et al., 2021a), we further assume that additional unlabeled data $\mathcal{D}_U (\subset \mathcal{D}_N)$ is available in the pre-training phase. We follow the split strategy used in Phoo & Hariharan (2021), where 20% of the target data \mathcal{D}_N is used as the unlabeled data \mathcal{D}_U for pre-training. Note that the size of the unlabeled portion is very small (*e.g.*, only a few thousand examples) compared to large-scale datasets typically considered for self-supervised learning.

In this problem setup, the pre-training phase of CD-FSL can be carried out based on *three* learning strategies:

- **Supervised Learning:** Let f and h_{sl} be the feature extractor and linear classifier for the base classes \mathcal{C}_B , respectively. Then, a model $h_{sl} \circ f$ is pre-trained only for the labeled source data \mathcal{D}_B by minimizing the standard cross-entropy loss ℓ_{ce} in a mini-batch manner¹,

$$\mathcal{L}_{sl}(f, h_{sl}; \mathcal{D}_B) = \frac{1}{|\mathcal{D}_B|} \sum_{(x,y) \in \mathcal{D}_B} \ell_{ce}(h_{sl} \circ f(x), y). \quad (1)$$

- **Self-Supervised Learning:** Let h_{ssl} be the projection head. Then, a model $h_{ssl} \circ f$ is pre-trained only for the unlabeled target data \mathcal{D}_U , which is much smaller than the labeled source data, by minimizing (non-)contrastive self-supervised loss ℓ_{self} (*e.g.*, NT-Xent)¹,

$$\begin{aligned} \mathcal{L}_{ssl}(f, h_{ssl}; \mathcal{D}_U) = \\ \frac{1}{2|\mathcal{D}_U|} \sum_{x \in \mathcal{D}_U} \left[\ell_{self}(z_1; z_2; \{z^-\}) + \ell_{self}(z_2; z_1; \{z^-\}) \right] \end{aligned} \quad (2)$$

where $z_i = h_{ssl} \circ f(A_i(x))$,

and $A_i(x)$ is the i -th augmentation of the same input x . This training loss forces z_1 to be similar to z_2 and dissimilar to the set of negative features $\{z^-\}$. In addition, there are non-contrastive SSL methods that do not rely on negative examples, *i.e.*, $\{z^-\} = \emptyset$. We provide a more detailed explanation of SSL losses, including multiple (non-)contrastive approaches in Appendix A.

- **Mixed-Supervised Learning:** MSL exploits labeled as well as unlabeled data from different domains simultaneously. Intuitively, MSL can be formulated by minimizing the convex interpolation of their losses in Eqs. (1) and (2),

$$\begin{aligned} \mathcal{L}_{msl}(f, h_{sl}, h_{ssl}; \mathcal{D}_B, \mathcal{D}_U) = \\ (1 - \gamma) \cdot \mathcal{L}_{sl}(f, h_{sl}; \mathcal{D}_B) + \gamma \cdot \mathcal{L}_{ssl}(f, h_{ssl}; \mathcal{D}_U), \end{aligned} \quad (3)$$

¹The batch loss on the entire data is used for ease of exposition.

where $0 < \gamma < 1$ and the feature extractor f is hard-shared and trained through SL and SSL losses with a balancing hyperparameter γ . This can be a generalization of STARTUP and Dynamic Distillation, which use Eq. (3) in the second pre-training phase with a moderate modification after the typical pre-training phase using SL.

Based on the three learning strategies, we conduct an empirical study to gain an in-depth understanding of their effectiveness in the pre-training phase, providing deep insight into the following questions:

1. Which is more effective for pre-training, using only SL or SSL? \triangleright Section 4
2. How to apply domain similarity and few-shot difficulty to identify the appropriate pre-training scheme, SL or SSL, for CD-FSL? \triangleright Section 5
3. Can MSL, a combination of SL and SSL, as well as a two-stage scheme improve performance? \triangleright Section 6

3.2. Domain Similarity and Few-Shot Difficulty

We present a procedure for estimating the two metrics on datasets, which are used to analyze the pre-training schemes. Inspired by Cui et al. (2018), we estimate the *domain similarity* between source and target data based on the Earth Mover’s Distance (EMD (Rubner et al., 1998)) using retrieved feature representations². We first create the prototype vector \mathbf{p}_i , which is the averaged vector of the representations for all examples belonging to class i . Next, let $i \in \mathcal{C}_B$ and $j \in \mathcal{C}_N$ be a class in base (source) and novel (target) classes, respectively. Then, the domain similarity between the source and target data is formulated as

$$\begin{aligned} \text{Sim}(\mathcal{D}_B, \mathcal{D}_N) &= \exp(-\alpha \text{EMD}(\mathcal{D}_B, \mathcal{D}_N)) \\ \text{where } \text{EMD}(\mathcal{D}_B, \mathcal{D}_N) &= \frac{\sum_{i \in \mathcal{C}_B, j \in \mathcal{C}_N} f_{i,j} d_{i,j}}{\sum_{i \in \mathcal{C}_B, j \in \mathcal{C}_N} f_{i,j}} \\ \text{subject to } f_{i,j} &\geq 0, \quad \sum_{i \in \mathcal{C}_B, j \in \mathcal{C}_N} f_{i,j} = 1, \\ \sum_{j \in \mathcal{C}_N} f_{i,j} &\leq \frac{|\mathcal{D}_B[i]|}{|\mathcal{D}_B|}, \quad \sum_{i \in \mathcal{C}_B} f_{i,j} \leq \frac{|\mathcal{D}_N[j]|}{|\mathcal{D}_N|}, \end{aligned} \quad (4)$$

and $d_{i,j} = \|\mathbf{p}_i - \mathbf{p}_j\|_2$; $f_{i,j}$ is the optimal flow between \mathbf{p}_i and \mathbf{p}_j subject to the constraints for EMD; $\mathcal{D}[i]$ returns all examples of the specified class i in \mathcal{D} ; and α is typically set to 0.01 (Cui et al., 2018). The larger similarity indicates that source and target data share similar domains.

Next, we propose *few-shot difficulty*, which quantifies the difficulty of a dataset based on the empirical upper bound of few-shot performance in our problem setup, regardless of their relationship to the source dataset. To capture the upper

bound of FSL performance, we use 20% of the target dataset as labeled data to pre-train the model in a supervised manner. Then, the pre-trained model is evaluated on the remaining unseen target data for the 5-way k -shot classification task³. As the generalization capability indicates the hardness (Song et al., 2020), the classification accuracy for unseen data is used and converted into the few-shot difficulty using an exponential function with a hyperparameter β (the default value is 0.01),

$$\text{Diff}(\mathcal{D}, k) = \exp(-\beta \text{Acc}(\mathcal{D}, k)), \quad (5)$$

where $\text{Acc}(\mathcal{D}, k)$ returns the average of 5-way k -shot classification accuracy over 600 episodes for the given data \mathcal{D} . Note that in our paper, k is set to 5, but the order of difficulty is the same regardless of k . The dataset with high few-shot difficulty exhibits lower few-shot accuracy even if the same domain data were used for pre-training as well as evaluation.

3.3. Experimental Configurations

Cross-Domain Datasets. We use ImageNet, tieredImageNet, and miniImageNet as source datasets for generality. Regarding the target domain, we prepare eight datasets with varying domain similarity and few-shot difficulty; domain similarity is computed based on both the source and target datasets, while few-shot difficulty is computed based on the target dataset. To summarize their order in Figure 1, **domain similarity**: *Places* $>$ *CUB* $>$ *Cars* $>$ *Plantae* $>$ *EuroSAT* $>$ *CropDisease* $>$ *ISIC* $>$ *ChestX*, and **few-shot difficulty**: *ChestX* $>$ *ISIC* $>$ *CUB* $>$ *Cars* $>$ *Plantae* $>$ *Places* $>$ *EuroSAT* $>$ *CropDisease*. For instance, Places data has the largest domain similarity to ImageNet, while ChestX has the highest few-shot difficulty among them. Appendix B provides the details of each dataset. The detailed values for domain similarity and few-shot difficulty are reported in Appendix D and E, respectively. These are visualized in Appendix F. We also provide the results on the case when source and target domains are the same (*i.e.*, the standard FSL setting) in Appendix M.

Evaluation Pipeline. We follow the evaluation pipeline of the standard CD-FSL (Guo et al., 2020). The evaluation process is performed in an episodic manner, where each episode represents a distinct few-shot task. Each episode is comprised of a support set \mathcal{D}_S and a query set \mathcal{D}_Q , which are sampled from the entire labeled target data \mathcal{D}_L . The support set \mathcal{D}_S and query set \mathcal{D}_Q consist of n classes that are randomly selected among the entire set of novel classes \mathcal{C}_N . For the n -way k -shot setting, k examples are randomly drawn from each class for the support set \mathcal{D}_S , while k_q (typically 15) examples for the query set \mathcal{D}_Q . Thus, the support and

²To extract the representation of examples in the source and target data, we use ResNet101 trained on ImageNet, publicly available in the PyTorch repository (Paszke et al., 2019).

³We use a few-shot learning task instead of classification on the entire data, preventing the performance from being distorted by other factors, such as data imbalance and the number of classes.

Table 2. 5-way k -shot CD-FSL performance (%) of the models pre-trained by SL and SSL. We report the average accuracy and its 95% confidence interval over 600 few-shot episodes. B and S indicate base and strong augmentation methods, respectively. The best accuracy is marked in bold for each backbone.

Source Data	Pre-train Scheme	Method	Aug.	EuroSAT		CropDisease		ISIC		ChestX	
				$k=1$	$k=5$	$k=1$	$k=5$	$k=1$	$k=5$	$k=1$	$k=5$
ImageNet	SL	Default	B	66.14±.83	84.73±.51	74.18±.82	92.81±.45	31.11±.55	44.10±.58	22.48±.39	25.51±.44
tiered ImageNet	SL	Default	B	61.81±.88	79.87±.67	66.82±.90	87.19±.59	30.35±.60	41.67±.55	22.34±.38	25.08±.45
			S	60.07±.88	79.95±.66	65.70±.94	86.34±.60	29.75±.56	40.60±.58	22.11±.42	25.20±.41
-	SSL	SimCLR	B	70.37±.86	87.80±.46	90.94±.69	97.44±.29	34.13±.69	44.37±.66	21.41±.41	25.05±.42
			S	84.30±.73	94.12±.32	91.00±.76	97.46±.34	36.39±.66	47.85±.65	21.55±.41	25.26±.44
		MoCo	B	51.21±.93	68.19±.74	70.22±.95	87.11±.60	27.79±.53	36.60±.59	21.44±.43	24.28±.43
			S	69.11±.98	81.01±.73	80.08±.97	92.48±.52	29.54±.59	39.28±.58	21.74±.42	24.58±.44
		BYOL	B	60.98±.91	84.88±.56	81.58±.78	96.82±.27	35.31±.64	49.26±.64	22.65±.42	28.80±.49
			S	66.16±.86	87.83±.48	85.77±.73	96.93±.30	34.53±.62	47.59±.63	22.75±.41	28.36±.46
		SimSiam	B	44.06±.86	61.03±.72	75.36±.82	92.31±.44	26.99±.52	35.68±.52	22.02±.41	26.06±.46
			S	70.80±.88	85.10±.57	84.72±.80	96.05±.36	30.17±.56	39.51±.55	22.17±.40	26.56±.46

(a) ResNet18 is used as a backbone.

mini ImageNet	SL	Default	B	64.03±.91	82.72±.59	73.38±.87	91.53±.49	30.68±.58	41.77±.59	22.64±.40	26.26±.45
			S	65.03±.88	84.00±.56	72.82±.87	91.32±.49	29.91±.54	40.84±.56	22.88±.42	27.01±.44
-	SSL	SimCLR	B	66.77±.84	86.39±.48	89.33±.66	96.82±.32	33.32±.63	44.50±.64	22.26±.42	24.34±.42
			S	79.50±.78	92.36±.37	89.49±.74	97.24±.33	34.90±.64	46.76±.61	21.97±.41	25.62±.43
		MoCo	B	48.70±.92	66.85±.72	68.77±.92	87.67±.57	27.76±.54	38.03±.57	21.55±.42	24.48±.44
			S	76.20±.89	89.54±.46	80.19±.99	93.41±.53	30.20±.55	41.14±.57	21.64±.40	24.49±.43
		BYOL	B	61.18±.82	83.11±.57	80.50±.75	94.85±.35	33.02±.62	46.72±.65	22.90±.41	27.40±.47
			S	66.45±.80	86.55±.50	80.10±.76	94.53±.41	33.50±.59	45.99±.63	23.11±.42	27.71±.44
		SimSiam	B	44.57±.82	63.67±.67	82.83±.73	95.37±.34	30.74±.60	41.28±.62	22.76±.42	27.50±.47
			S	71.66±.88	85.21±.59	81.25±.77	95.13±.37	31.80±.59	41.44±.59	23.22±.41	27.83±.46

(b) ResNet10 is used as a backbone.

query set are defined as,

$$\mathcal{D}_S = \{(x_i^s, y_i^s)\}_{i=1}^{n \times k} \text{ and } \mathcal{D}_Q = \{(x_i^q, y_i^q)\}_{i=1}^{n \times k_q}. \quad (6)$$

For evaluation, a classifier g is fine-tuned on the support set \mathcal{D}_S , using features extracted from the fixed pre-trained backbone f . Note that g is for the evaluation purpose different from h_{sl} and h_{ssl} for pre-training. The fine-tuned model $g \circ f$ is then tested on the query set \mathcal{D}_Q . We set $n = 5$ and $k = \{1, 5\}$ following convention. The accuracy averaged over 600 episodes is a common measure of CD-FSL (Guo et al., 2020; Phoo & Hariharan, 2021).

Implementation. We use different backbone networks depending on the source data. For tieredImageNet and ImageNet, ResNet18 is used as the backbone, while ResNet10 is used for miniImageNet. ResNet18 trained on ImageNet trained by SL is downloaded on the PyTorch (Paszke et al., 2019) repository. This setup is exactly the same for all pre-training schemes. Additional details on the training setup are provided in Appendix C.

4. Supervised Learning on Source vs. Self-Supervised Learning on Target Data

We begin by investigating the superiority of SSL over SL for pre-training. We compared the CD-FSL performance of pre-trained models using four existing SSL methods (SimCLR

(Chen et al., 2020a), MoCo (He et al., 2020), BYOL (Grill et al., 2020), and SimSiam (Chen & He, 2021)) with that of a supervised learning method (Default) in Table 2; four different domain datasets from the BSCD-FSL benchmarks (EuroSAT, CropDisease, ISIC, and ChestX) are used as target data for each source data. Table 2 provides empirical evidence of all the findings in this section. Recent literature has reported that SSL pre-training does *not* work better than SL for the CD-FSL task because of insufficient unlabeled examples of target domain (Phoo & Hariharan, 2021; Islam et al., 2021a). However, our observation contradicts the previous finding.

OBSERVATION 4.1. *SSL on the target domain can achieve remarkably higher performance over SL on the labeled source domain, even with small-scale unlabeled target data (i.e., a few thousand examples).*

EVIDENCE. SSL methods are observed to outperform the SL method in most cases, even though SSL does not leverage source data for pre-training. In particular, the SSL methods show much higher performance compared to the model pre-trained on the entire ImageNet dataset, which has more than 1M training examples. This leads to the conclusion that SSL on the target domain can be better than SL on the source domain to build a pre-trained model for CD-FSL. In other words, unlabeled target data available at the pre-training phase is worth more than labeled source data, even if the

unlabeled target data is much smaller (e.g., 8k examples for CropDisease) than the labeled source data. We further provide the results of using a smaller ratio of unlabeled target data in Appendix G.

OBSERVATION 4.2. *SSL achieves significant performance gains with strong data augmentation.*

EVIDENCE. In addition, the results in Table 2 provide the performance sensitivity to data augmentation. For this study, two types of augmentation are used: (1) base augmentation (Chen et al., 2020a), which consists of random resized crop, color jitter, horizontal flip, and normalization, and (2) strong augmentation (Islam et al., 2021a), which adds Gaussian blur and random gray scale to the base (see the detail of the augmentations in Appendix C). With strong augmentation, SSL methods exhibit significant performance gains of up to 27.09%p compared to base augmentation. However, the SL method with strong augmentation does not experience the improvement that SSL does. This has been also observed in the recent literature (Chen et al., 2020a). Therefore, unlike SL, the performance of SSL can be further improved for CD-FSL if more suitable augmentation is applied. Based on this observation, we use strong augmentation for SSL as the default setup in the rest of our paper.

OBSERVATION 4.3. *SimCLR, one of the contrastive methods, achieves the best CD-FSL performance in most cases. BYOL, one of the non-contrastive methods, has comparable or better performance than the contrastive methods under high few-shot difficulty (e.g., ISIC and ChestX).*

EVIDENCE. The SSL methods can be categorized into two groups for comparison, i.e., contrastive learning: SimCLR and MoCo, and non-contrastive learning: BYOL and SimSiam. Each group is observed to have a more favorable CD-FSL environment depending on the few-shot difficulty. When we compare contrastive and non-contrastive methods, few-shot difficulty becomes an important factor in determining which SSL approach is more effective for pre-training. For the contrastive SSL, the ability to contrast the positive example with negative examples is crucial. This implies that if it is difficult to distinguish the instances (i.e., hard-to-contrast), contrastive methods may struggle to extract more meaningful representations than non-contrastive methods. Therefore, on datasets with high few-shot difficulty (refer to the difficulty order in Section 3.3), non-contrastive methods are promising because they do not rely on negative examples. The results for other target datasets are presented in Appendix H.

5. Closer Look at Domain Similarity and Few-Shot Difficulty

In this section, we investigate how domain similarity and few-shot difficulty in Eqs. (4) and (5) affect the perfor-

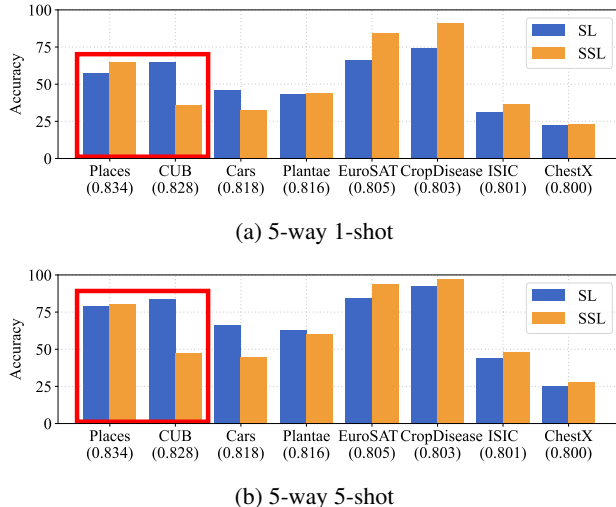


Figure 2. 5-way k -shot CD-FSL performance (%) of SL and SSL according to domain similarity (values in x-axis), with ImageNet source data. SimCLR is used for all datasets except ChestX, for which BYOL is used. The red box shows that SL outperforms SSL in the second highest domain similarity, while SSL outperforms SL in the highest domain similarity.

mance of pre-trained models. We analyze existing benchmark datasets by the two metrics and provide insights for developing a more effective pre-training approach.

Including BSCD-FSL, we consider four additional datasets from different domains: Places, CUB, Cars, and Plantae. We mainly use ImageNet as the source dataset to make our analysis more reliable. We analyze their domain similarity and few-shot difficulty and display them in Figure 1, where ImageNet is used as source data for domain similarity.

5.1. Domain Similarity

Figure 2 shows the CD-FSL performance of the pre-trained models using SL and SSL for eight datasets with varying domain similarity, where all the datasets are sorted by domain similarity. A common belief about domain similarity is that, as domain similarity increases, it is more beneficial for pre-training to use a large number of labeled source data. Our analysis shows that this belief is only partially true.

OBSERVATION 5.1. *There is no consistent performance benefit for SL according to the domain similarity.*

EVIDENCE. For the aforementioned belief to be true, the performance gain of SL over SSL should be greater as domain similarity increases. However, although SL outperforms SSL in the CUB dataset with the second highest domain similarity, in the Places dataset with the largest domain similarity, SSL rather exhibits higher CD-FSL accuracy than SL (see the red box in Figure 2). Namely, it seems to be true that SSL is a better strategy when the target domain is dissimilar to the source domain (Observation 4.1), but the

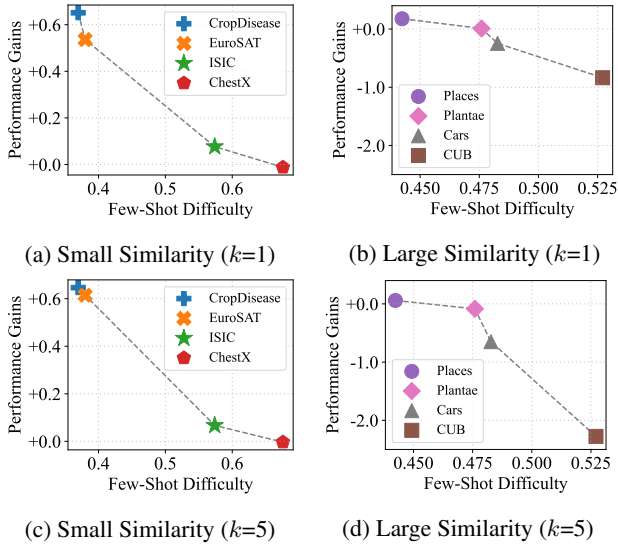


Figure 3. 5-way k -shot performance gain of SSL over SL for the two dataset groups according to the few-shot difficulty. ImageNet is used as the source dataset. SimCLR is used for all datasets except ChestX, for which BYOL is used.

superiority of SSL on Places cannot be explained solely by domain similarity.

5.2. Few-Shot Difficulty

In this sense, we study the impact of few-shot difficulty by categorizing the eight datasets into two groups, one with small domain similarity (*i.e.*, BSCD-FSL) and another with large domain similarity (*i.e.*, other datasets). Figure 3 shows the performance gain of SSL over SL for datasets with varying few-shot difficulty for each group. The performance gain of SSL over SL is defined as $(\text{Error}_{\text{sl}} - \text{Error}_{\text{ssl}}) / \text{Error}_{\text{sl}}$, which indicates the relative improvement of the classification error. Note that the negative value of performance gain means that SL outperforms SSL.

OBSERVATION 5.2. *Performance gain of SSL over SL becomes greater at smaller domain similarity or lower few-shot difficulty.*

EVIDENCE. When comparing the two groups (BSCD-FSL vs. other datasets), it is observed that the performance gain is more significant for the group with small domain similarity. Meanwhile, for both groups, the performance gain of SSL over SL becomes greater as few-shot difficulty decreases. In particular, the performance gain is the greatest on the CropDisease and Places datasets with the lowest few-shot difficulty in each group, while the performance gain is the least on the ChestX and CUB datasets with the highest few-shot difficulty in each group. For the target data with higher few-shot difficulty, it may not be easy to learn discriminative representations by solely using SSL without label supervision.

In summary, we first conclude that SSL is advantageous to SL when the target domain is extremely dissimilar to the source domain, which is in line with Observation 4.1. However, when domain similarity is large, few-shot difficulty must be considered to determine the performance gain through SSL. Namely, target datasets with higher few-shot difficulty exhibit less performance gain of SSL over SL.

As shown in Figure 3, when domain similarity is large, the performance gain is near or less than zero. This is related to the source dataset size, explained in Appendix I. Furthermore, inspired by the observations above, we consider schemes to maximize the utilization of the source dataset in the next section.

6. Advanced Scheme: MSL and Two-Stage

In this section, we further study SL and SSL in a more advanced scheme, which can be explained from the domain similarity and few-shot difficulty perspective, in line with previous observations. We first investigate whether SL and SSL can synergize by studying MSL. Next, we analyze two-stage pre-training scheme used in recent works (Phoo & Hariharan, 2021; Islam et al., 2021a).

6.1. Can SL and SSL Synergize?

The two schemes of SL and SSL can be combined as MSL in Eq. (3) for pre-training. To identify whether SL and SSL complement each other, we compare the performance of MSL to that of SL and SSL, respectively. We assume that synergy between SL and SSL occurs if MSL is superior to both SL and SSL. Table 3(a) summarizes the CD-FSL performance of the models pre-trained by SL, SSL, and MSL on the eight benchmark datasets grouped by their domain similarity (BSCD-FSL vs. other datasets) and then sorted by few-shot difficulty in ascending order in each group. In MSL, a hyperparameter γ is set to be 0.875 found by a grid search, detailed in Appendix J.

OBSERVATION 6.1. *SL and SSL do not always synergize.*

EVIDENCE. SSL supports SL ($\text{MSL} > \text{SL}$) for six datasets (CropDisease, EuroSAT, ISIC, ChestX, Places, and Plantae). This is in line with Observation 5.2 that SSL becomes a better pre-training strategy than SL when domain similarity is small (CropDisease, EuroSAT, ISIC, and ChestX) or few-shot difficulty is low (CropDisease, EuroSAT, Places, and Plantae). On the other hand, SL supports SSL ($\text{MSL} > \text{SSL}$) for six datasets (ISIC, ChestX, Places, Plantae, Cars, and CUB). This is in line with Observation 5.1 that there is no consistent benefit from using SL even when the target domain gets more similar to the source domain (*e.g.*, CropDisease vs. ChestX). In summary, SL and SSL have synergy when both conditions are extreme, *i.e.*, small similarity/high difficulty (ISIC and ChestX) or large similarity/low difficulty (Places and Plantae).

Table 3. 5-way 5-shot CD-FSL performance (%) of the models pre-trained by SL, SSL, and MSL including their two-stage versions. ResNet18 is used as the backbone model, and ImageNet is used as the source data for SL and MSL. The balancing coefficient γ in Eq. (3) of MSL is set to be 0.875. Datasets grouped by domain similarity and sorted by few-shot difficulty in ascending order in each group (CropDisease < ChestX | Places < CUB). STARTUP results are from Phoo & Hariharan (2021). The best results are marked in bold.

	Pre-train Scheme	Method	Small Similarity				Large Similarity			
			CropDisease	EuroSAT	ISIC	ChestX	Places	Plantae	Cars	CUB
Single-Stage	SL	Default	92.81±.45	84.73±.51	44.10±.58	25.51±.44	79.22±.64	63.21±.82	66.38±.80	83.93±.66
	SSL	SimCLR	97.46±.34	94.12±.32	47.85±.65	25.26±.44	80.43±.61	60.07±.84	44.55±.74	47.36±.79
		BYOL	96.93±.30	87.83±.48	47.59±.63	28.36±.46	72.47±.63	61.02±.82	48.56±.76	51.31±.78
	MSL	SimCLR	96.50±.35	90.11±.40	45.38±.63	26.05±.44	82.56±.58	64.76±.83	51.84±.79	64.53±.80
		BYOL	96.74±.31	90.82±.40	49.14±.70	29.58±.47	81.27±.59	67.39±.81	46.76±.73	69.67±.82
	(a) Performance comparison for single-stage schemes.									
Two-Stage	SL→SSL	SimCLR	97.88±.30	95.28±.27	48.38±.60	25.25±.44	84.40±.53	66.35±.82	51.31±.84	57.11±.88
		BYOL	97.58±.26	91.82±.39	49.32±.63	28.27±.48	78.87±.60	67.83±.82	54.70±.84	60.60±.82
	SL→MSL	SimCLR	97.49±.30	91.70±.35	47.43±.62	26.24±.44	85.76±.52	69.24±.81	58.97±.82	81.51±.72
		BYOL	97.09±.31	90.89±.40	50.72±.67	30.20±.48	83.29±.55	74.16±.77	68.87±.80	84.34±.67
	SL→MSL ⁺	STARTUP	96.06±.33	89.70±.41	46.02±.59	27.24±.46	-	-	-	-
(b) Performance comparison for two-stage schemes.										

In addition, when SL can support SSL, domain similarity becomes an important factor to determine the performance gain of MSL over SSL, $(\text{Error}_{\text{ssl}} - \text{Error}_{\text{msl}}) / \text{Error}_{\text{ssl}}$ ⁴, and the improvement is considerable when domain similarity is large. Performance gain is only +0.024 on average for datasets with small domain similarity, *i.e.*, ISIC and ChestX, but reaches +0.248 on average for datasets with large domain similarity, *i.e.*, Places, Plantae, Cars, and CUB. Furthermore, MSL performance can be improved by increasing the batch size (Appendix K).

6.2. Extension to Two-Stage Approach

We extend the single-stage MSL into the two-stage approaches, extracting more sophisticated target representations. In two-stage pre-training, a model is pre-trained *in prior* with labeled source data in the first phase and further trained through SSL or MSL in the second phase, *i.e.*, SL → SSL or SL → MSL. This pipeline has been adopted by recent algorithms, such as STARTUP (Phoo & Hariharan, 2021) and Dynamic Distillation (Islam et al., 2021a), but they additionally maintain an extra network or incorporate the knowledge distillation in the second phase, *i.e.*, SL → MSL⁺. We examine the effectiveness of these two-stage approaches for CD-FSL. Table 3(b) summarizes the CD-FSL performance of using them for pre-training.

OBSERVATION 6.2. *The two-stage pre-training scheme is more powerful than single-stage counterparts.*

EVIDENCE. Two-stage pre-training approaches achieve much higher performance than all their single-stage counterparts in general, *i.e.*, SL → SSL outperforms SSL, and SL → MSL outperforms MSL. When SL is used separately at

⁴Between SimCLR and BYOL, the larger improvement is considered.

the first phase, it appears to provide a good initialization for the second phase. It is known that a converged extractor on the source data is better than a random extractor (Neyshabur et al., 2020). Therefore, with the two-stage scheme, we can benefit from the first-stage SL on all datasets, regardless of domain similarity and few-shot difficulty. The benefit of two-stage is significant when domain similarity is large. This observation is significantly promising for practitioners because pre-trained models on ImageNet or bigger datasets are readily accessible. In addition, our simple two-stage methods, without any additional techniques, are shown to achieve better performance than the meticulously designed two-stage approaches such as STARTUP, even though our main goal is analysis on basic pre-training methods. 5-way 1-shot and additional experimental results with other source datasets are presented in Appendix L, which show consistent results as ImageNet experiments.

7. Conclusion

We established a thorough empirical understanding of CD-FSL. In particular, we mainly focused on the effectiveness of SL, SSL, and MSL, which can be realized with single- and two-stage pre-training schemes. Their performances are closely related to (1) domain similarity between the source and target datasets and few-shot difficulty of the provided target dataset, and (2) how they are combined for pre-training. Through our empirical study, we present seven findings that have been either misunderstood or unexplored. To justify all the findings, extensive experiments were conducted on benchmark datasets with varying degrees of domain similarity and few-shot difficulty. Overall, we believe that our work unveils many hidden findings and can inspire subsequent studies for CD-FSL.

References

- Andrychowicz, M., Denil, M., Gomez, S., Hoffman, M. W., Pfau, D., Schaul, T., Shillingford, B., and De Freitas, N. Learning to learn by gradient descent by gradient descent. In *NeurIPS*, 2016.
- Caron, M., Misra, I., Mairal, J., Goyal, P., Bojanowski, P., and Joulin, A. Unsupervised learning of visual features by contrasting cluster assignments. *arXiv preprint arXiv:2006.09882*, 2020.
- Chen, T., Kornblith, S., Norouzi, M., and Hinton, G. A simple framework for contrastive learning of visual representations. In *ICML*, 2020a.
- Chen, W.-Y., Liu, Y.-C., Kira, Z., Wang, Y.-C. F., and Huang, J.-B. A closer look at few-shot classification. In *ICLR*, 2019.
- Chen, X. and He, K. Exploring simple siamese representation learning. In *CVPR*, 2021.
- Chen, X., Fan, H., Girshick, R., and He, K. Improved baselines with momentum contrastive learning. *arXiv preprint arXiv:2003.04297*, 2020b.
- Codella, N., Rotemberg, V., Tschandl, P., Celebi, M. E., Dusza, S., Gutman, D., Helba, B., Kalloo, A., Liopyris, K., Marchetti, M., et al. Skin lesion analysis toward melanoma detection 2018: A challenge hosted by the international skin imaging collaboration (isic). *arXiv preprint arXiv:1902.03368*, 2019.
- Cole, E., Yang, X., Wilber, K., Mac Aodha, O., and Belongie, S. When does contrastive visual representation learning work? *arXiv preprint arXiv:2105.05837*, 2021.
- Cui, Y., Song, Y., Sun, C., Howard, A., and Belongie, S. Large scale fine-grained categorization and domain-specific transfer learning. In *CVPR*, 2018.
- Deng, J., Dong, W., Socher, R., Li, L.-J., Li, K., and Fei-Fei, L. ImageNet: A large-scale hierarchical image database. In *CVPR*, 2009.
- Dhillon, G. S., Chaudhari, P., Ravichandran, A., and Soatto, S. A baseline for few-shot image classification. In *ICLR*, 2020.
- Doersch, C., Gupta, A., and Efros, A. A. Unsupervised visual representation learning by context prediction. In *ICCV*, 2015.
- Dosovitskiy, A., Fischer, P., Springenberg, J. T., Riedmiller, M., and Brox, T. Discriminative unsupervised feature learning with exemplar convolutional neural networks. *IEEE Transactions on Pattern Analysis and Machine Intelligence*, 38(9):1734–1747, 2015.
- Ericsson, L., Gouk, H., and Hospedales, T. M. How well do self-supervised models transfer? In *CVPR*, 2021.
- Finn, C., Abbeel, P., and Levine, S. Model-agnostic meta-learning for fast adaptation of deep networks. In *ICML*, 2017.
- Finn, C., Xu, K., and Levine, S. Probabilistic model-agnostic meta-learning. *arXiv preprint arXiv:1806.02817*, 2018.
- Flennerhag, S., Rusu, A. A., Pascanu, R., Visin, F., Yin, H., and Hadsell, R. Meta-learning with warped gradient descent. In *ICLR*, 2020.
- Gidaris, S., Singh, P., and Komodakis, N. Unsupervised representation learning by predicting image rotations. In *ICLR*, 2018.
- Grill, J.-B., Strub, F., Altché, F., Tallec, C., Richemond, P. H., Buchatskaya, E., Doersch, C., Pires, B. A., Guo, Z. D., Azar, M. G., et al. Bootstrap your own latent: A new approach to self-supervised learning. *arXiv preprint arXiv:2006.07733*, 2020.
- Guo, Y., Codella, N. C., Karlinsky, L., Codella, J. V., Smith, J. R., Saenko, K., Rosing, T., and Feris, R. A broader study of cross-domain few-shot learning. In *ECCV*, 2020.
- He, K., Fan, H., Wu, Y., Xie, S., and Girshick, R. Momentum contrast for unsupervised visual representation learning. In *CVPR*, 2020.
- Helber, P., Bischke, B., Dengel, A., and Borth, D. Eurosat: A novel dataset and deep learning benchmark for land use and land cover classification. *IEEE Journal of Selected Topics in Applied Earth Observations and Remote Sensing*, 12(7):2217–2226, 2019.
- Hinton, G., Vinyals, O., and Dean, J. Distilling the knowledge in a neural network. In *NeurIPS*, 2015.
- Islam, A., Chen, C.-F., Panda, R., Karlinsky, L., Feris, R., and Radke, R. J. Dynamic distillation network for cross-domain few-shot recognition with unlabeled data. *arXiv preprint arXiv:2106.07807*, 2021a.
- Islam, A., Chen, C.-F., Panda, R., Karlinsky, L., Radke, R., and Feris, R. A broad study on the transferability of visual representations with contrastive learning. *arXiv preprint arXiv:2103.13517*, 2021b.
- Kim, D., Saito, K., Oh, T.-H., Plummer, B. A., Sclaroff, S., and Saenko, K. Cds: Cross-domain self-supervised pre-training. In *ICCV*, 2021.
- Kingma, D. P. and Ba, J. Adam: A method for stochastic optimization. *arXiv preprint arXiv:1412.6980*, 2014.

- Krause, J., Stark, M., Deng, J., and Fei-Fei, L. 3d object representations for fine-grained categorization. In *ICCVW*, 2013.
- Lee, K., Maji, S., Ravichandran, A., and Soatto, S. Meta-learning with differentiable convex optimization. In *CVPR*, 2019.
- Li, H., Chaudhari, P., Yang, H., Lam, M., Ravichandran, A., Bhotika, R., and Soatto, S. Rethinking the hyperparameters for fine-tuning. *arXiv preprint arXiv:2002.11770*, 2020.
- Maclaurin, D., Duvenaud, D., and Adams, R. Gradient-based hyperparameter optimization through reversible learning. In *ICML*, 2015.
- Mohanty, S. P., Hughes, D. P., and Salathé, M. Using deep learning for image-based plant disease detection. *Frontiers in Plant Science*, 7:1419, 2016.
- Neyshabur, B., Sedghi, H., and Zhang, C. What is being transferred in transfer learning? *arXiv preprint arXiv:2008.11687*, 2020.
- Noroozi, M. and Favaro, P. Unsupervised learning of visual representations by solving jigsaw puzzles. In *ECCV*, pp. 69–84. Springer, 2016.
- Noroozi, M., Pirsivash, H., and Favaro, P. Representation learning by learning to count. In *ICCV*, pp. 5898–5906, 2017.
- Oh, J., Yoo, H., Kim, C., and Yun, S.-Y. BOIL: Towards representation change for few-shot learning. In *ICLR*, 2021.
- Pan, S. J. and Yang, Q. A survey on transfer learning. *IEEE Transactions on Knowledge and Data Engineering*, 22(10):1345–1359, 2009.
- Paszke, A., Gross, S., Massa, F., Lerer, A., Bradbury, J., Chanan, G., Killeen, T., Lin, Z., Gimelshein, N., Antiga, L., Desmaison, A., Kopf, A., Yang, E., DeVito, Z., Raison, M., Tejani, A., Chilamkurthy, S., Steiner, B., Fang, L., Bai, J., and Chintala, S. Pytorch: An imperative style, high-performance deep learning library. In Wallach, H., Larochelle, H., Beygelzimer, A., d'Alché-Buc, F., Fox, E., and Garnett, R. (eds.), *NeurIPS*. 2019.
- Pathak, D., Krahenbuhl, P., Donahue, J., Darrell, T., and Efros, A. A. Context encoders: Feature learning by inpainting. In *CVPR*, pp. 2536–2544, 2016.
- Phoo, C. P. and Hariharan, B. Self-training for few-shot transfer across extreme task differences. In *ICLR*, 2021.
- Raghu, A., Raghu, M., Bengio, S., and Vinyals, O. Rapid learning or feature reuse? towards understanding the effectiveness of maml. *arXiv preprint arXiv:1909.09157*, 2019.
- Ravi, S. and Larochelle, H. Optimization as a model for few-shot learning. In *ICLR*, 2016.
- Ren, M., Triantafillou, E., Ravi, S., Snell, J., Swersky, K., Tenenbaum, J. B., Larochelle, H., and Zemel, R. S. Meta-learning for semi-supervised few-shot classification. *arXiv preprint arXiv:1803.00676*, 2018.
- Rubner, Y., Tomasi, C., and Guibas, L. J. A metric for distributions with applications to image databases. In *Sixth International Conference on Computer Vision (IEEE Cat. No. 98CH36271)*, pp. 59–66. IEEE, 1998.
- Snell, J., Swersky, K., and Zemel, R. S. Prototypical networks for few-shot learning. *arXiv preprint arXiv:1703.05175*, 2017.
- Sohn, K., Berthelot, D., Carlini, N., Zhang, Z., Zhang, H., Raffel, C. A., Cubuk, E. D., Kurakin, A., and Li, C.-L. Fixmatch: Simplifying semi-supervised learning with consistency and confidence. In *NeurIPS*, 2020.
- Song, H., Kim, M., Kim, S., and Lee, J.-G. Carpe diem, seize the samples uncertain” at the moment” for adaptive batch selection. In *CIKM*, 2020.
- Sung, F., Yang, Y., Zhang, L., Xiang, T., Torr, P. H., and Hospedales, T. M. Learning to compare: Relation network for few-shot learning. In *CVPR*, 2018.
- Tian, Y., Krishnan, D., and Isola, P. Contrastive multiview coding. In *CECCV*, 2020a.
- Tian, Y., Wang, Y., Krishnan, D., Tenenbaum, J. B., and Isola, P. Rethinking few-shot image classification: a good embedding is all you need? In *ECCV*, 2020b.
- Tseng, H.-Y., Lee, H.-Y., Huang, J.-B., and Yang, M.-H. Cross-domain few-shot classification via learned feature-wise transformation. In *ICLR*, 2020.
- Van Horn, G., Mac Aodha, O., Song, Y., Cui, Y., Sun, C., Shepard, A., Adam, H., Perona, P., and Belongie, S. The inaturalist species classification and detection dataset. In *CVPR*, 2018.
- Vinyals, O., Blundell, C., Lillicrap, T., Wierstra, D., et al. Matching networks for one shot learning. In *NeurIPS*, 2016.
- Wang, T. and Isola, P. Understanding contrastive representation learning through alignment and uniformity on the hypersphere. In *ICML*, 2020.

- Wang, X., Peng, Y., Lu, L., Lu, Z., Bagheri, M., and Summers, R. M. ChestX-ray8: Hospital-scale chest x-ray database and benchmarks on weakly-supervised classification and localization of common thorax diseases. In *CVPR*, 2017.
- Wang, Y., Yao, Q., Kwok, J. T., and Ni, L. M. Generalizing from a few examples: A survey on few-shot learning. *ACM Computing Surveys (CSUR)*, 53(3):1–34, 2020.
- Welinder, P., Branson, S., Mita, T., Wah, C., Schroff, F., Belongie, S., and Perona, P. Caltech-UCSD Birds 200. Technical Report CNS-TR-2010-001, California Institute of Technology, 2010.
- Zhang, R., Isola, P., and Efros, A. A. Colorful image colorization. In *ECCV*, 2016.
- Zhang, W., Deng, L., Zhang, L., and Wu, D. Overcoming negative transfer: A survey. *arXiv preprint arXiv:2009.00909*, 2020.
- Zhou, B., Lapedriza, A., Khosla, A., Oliva, A., and Torralba, A. Places: A 10 million image database for scene recognition. *IEEE Transactions on Pattern Analysis and Machine Intelligence*, 40(6):1452–1464, 2017.

A. Self-Supervised Learning Methods

A.1. SimCLR

SimCLR (Chen et al., 2020a) is one of the simplest yet high-performance contrastive learning method. Its key idea is mapping the semantically similar examples to be close in the representation space, while dissimilar examples to be distant. The similar examples are often called positive samples and the dissimilar ones are called negative samples. Formally, all examples in the current batch $\{x_k\}_{k=1:B}$ with size B are augmented to generate an augmented batch $\{\tilde{x}_{2k-1}, \tilde{x}_{2k}\}_{k=1:B}$, where \tilde{x}_{2k-1} and \tilde{x}_{2k} are the examples differently augmented from the same input x_k . Then, the representations $\{z_{2k-1}, z_{2k}\}_{k=1:B}$ are extracted from a feature extractor with projection layers. Based on the representations, SimCLR performs contrastive learning such that it minimizes the contrastive loss:

$$\mathcal{L}_{\text{SimCLR}} = \frac{1}{2B} \sum_{k=1}^B \left[\ell(2k-1, 2k) + \ell(2k, 2k-1) \right]$$

$$\text{where } \ell(i, j) = -\log \frac{\exp(\text{sim}(z_i, z_j)/\tau)}{\sum_{n=1}^{2B} \mathbf{1}_{[n \neq i]} \exp(\text{sim}(z_i, z_n)/\tau)}$$

where $\mathbf{1}$ is an indicator function, τ is a temperature hyperparameter, and $\text{sim}(\mathbf{u}, \mathbf{v}) = \frac{\mathbf{u}^\top \mathbf{v}}{\|\mathbf{u}\| \|\mathbf{v}\|}$ measures cosine similarity between two vectors \mathbf{u} and \mathbf{v} .

A.2. MoCo

MoCo (Momentum Contrast (He et al., 2020)) is a variant of SimCLR method, which leverages the memory bank and the momentum update of an encoder. Similar to SimCLR, MoCo also minimizes the contrastive loss with positive and negative samples; positive sample is the other augmentation (view) from the same instance, but the negative samples are not those from the current batch. Instead, MoCo fetches the negative samples from the memory bank, which has been enqueued from the previous batches. To emphasize the usage of memory bank, the anchor sample which is contrasted by positive and negative samples is called query q , while the others are called keys $\{k_0, k_1, \dots, k_K\}$. A positive key k_0 is the augmentation from the same sample as q . Then, MoCo minimizes the following contrastive loss:

$$\mathcal{L}_{\text{MoCo}} = -\frac{1}{B} \sum_{i=1}^B \log \frac{\exp(\text{sim}(q(i), k_0(i))/\tau)}{\sum_{j=0}^K \exp(\text{sim}(q(i), k_j(i))/\tau)}$$

where the query representation and the key representations are extracted from different models. That is, $q = f_q(x_q)$ where f_q is a main encoder, while $k = f_k(x_k)$ where f_k is a momentum encoder that is updated by the moving average of its previous state and that of f_q . MoCo overcomes the dependency of the negative sample size on batch size, efficiently achieving the objective of SimCLR using the small memory bank and the additional network.

There are two versions of MoCo: MoCo-v1 (He et al., 2020) and MoCo-v2 (Chen et al., 2020b). Since MoCo-v2 is a simple improvement of MoCo-v1, such as cosine annealing, MLP projector, and different hyperparameters, we only considered the MoCo-v1 version in this paper.

A.3. BYOL

While SimCLR and MoCo used positive and negative samples to construct a contrastive task, BYOL (Bootstrap Your Own Latent (Grill et al., 2020)) achieves higher performances than state-of-the-art contrastive learning models, without using the negative samples. That is, BYOL is a non-contrastive SSL method, completely free from the need of negative samples. To this end, BYOL minimizes a similarity loss between the two augmented views using two networks.

There are two networks involved: online network f_θ and target network f_ξ . This is a similar setting to MoCo; the online network is a main encoder and the target network is an encoder that is updated by weighted moving average. Given an image x , it augments x into two views \tilde{x} and \tilde{x}' . Each view is represented by the encoder with a projector g_θ and g_ξ : $z_\theta = g_\theta(f_\theta(\tilde{x}))$ and $z'_\xi = g_\xi(f_\xi(\tilde{x}'))$. Then, by prediction layers q_θ , a prediction $q_\theta(z_\theta)$ is output and it is compared with the target projection. BYOL uses a mean squared error between the normalized prediction and target projection:

$$\mathcal{L}_{\text{BYOL}} = 2 - 2 \cdot \frac{\langle q_\theta(z_\theta), z'_\xi \rangle}{\|q_\theta(z_\theta)\|_2 \cdot \|z'_\xi\|_2}$$

BYOL also uses a symmetric loss function which passes \tilde{x}' through the online network and \tilde{x} through the target network. The two losses are summed and the same thing is done for every sample in a batch.

A.4. SimSiam

SimSiam (Simple Siamese (Chen & He, 2021)) basically shares the similar idea to the BYOL model. The loss form is exactly the same, but SimSiam does not use an extra target network that is updated by momentum. Instead, SimSiam uses the same online network f_θ to output the representation of the two views \tilde{x}, \tilde{x}' , but blocks the gradient flow for the target projection. While Grill et al. (2020) insisted in BYOL the importance of a momentum encoder since it can prevent collapsing, Chen & He (2021) found that a stop-gradient operation is a key to avoid collapsing. Thus, SimSiam loss is described as follows:

$$\mathcal{L}_{\text{SimSiam}} = 2 - 2 \cdot \frac{\langle q_\theta(z_\theta), \text{sg}(q_\theta(z'_\theta)) \rangle}{\|q_\theta(z_\theta)\|_2 \cdot \|\text{sg}(q_\theta(z'_\theta))\|_2}$$

where sg indicates the stop-gradient operation.

B. Datasets Details

B.1. Datasets

In this paper, we used two source domain datasets and eight target domain datasets. Table 4 summarizes the referenced papers, number of classes, and number of samples of each dataset. For source domain datasets, we used miniImageNet and tieredImageNet, which are two different subsets of the ImageNet-1k dataset (Deng et al., 2009). The source dataset for miniImageNet (miniImageNet-train) includes 64 base classes, while the target dataset for miniImageNet (miniImageNet-test) include 20 classes that are disjoint from miniImageNet-train, following Appendix M. Similarly, tieredImageNet is partitioned into train and test set for the source data and target data, respectively. In our FSL experiments, we also reported the performance of SL model pre-trained on ImageNet. However, we did not actually pre-train with the ImageNet dataset, but fine-tuned from the pre-trained model offered by an official PyTorch (Paszke et al., 2019) library.

The target domain datasets can be separated into two groups: BSCD-FSL benchmark (Guo et al., 2020) and non-BSCD-FSL. First, BSCD-FSL benchmark include CropDisease, EuroSAT, ISIC, and ChestX. These datasets are *supposed* to be distant from miniImageNet source, with CropDisease most similar and ChestX most dissimilar. The criterion are perspective distortion, semantic contents, and color depth. We followed Phoo & Hariharan (2021) for the splitting procedure of target dataset into a pre-training unlabeled set and a few-shot evaluation set. A short description of each dataset is provided below.

- **CropDisease** is a set of diseased plant images.
- **EuroSAT** is a set of satellite images of the landscapes.
- **ISIC** is a set of dermoscopy images of human skin lesions.
- **ChestX** is a set of X-Ray images on the human chest.

In addition to the BSCD-FSL benchmark, we introduced four target datasets that are more commonly used in the (CD-)FSL literature. They are Places, Plantae, Cars and CUB. However, there is no standard rule to separate the pre-training set and the evaluation set for these four datasets. Thus, we sampled the images from each dataset. A short description and the sampling strategy of dataset is provided below. Also, for the reproducibility of our work, we provide the code for sampling procedure and the list of images we used.

- **Places** contains the images designed for scene recognition, such as bedrooms and streets, etc. However, since Places is an enormous dataset to use in the FSL context, we sampled 16 classes out of 365 classes (in total of train, val, and test). Also, to make the dataset size smaller, we sampled 1,715 images per class, which is a reduced amount from the original 4,941 images per class in average.
- **Plantae** contains the plant images. Similar to Places, we sampled some images to reduce the dataset size. However, unlike Places, Plantae is a highly class-imbalanced set. Therefore, we sampled top 69 classes that have many samples out of 2,917 classes.
- **Cars** contains the images of 196 car models. We used the entire images that Cars dataset has (train and test).
- **CUB** contains the images of 200 species of birds. We used the entire images that CUB dataset has (train, val, and test).

Table 4. Summary of datasets we used in this paper. Note that we used a subset of images for Places and Plantae dataset.

Datasets	miniImageNet-train	miniImageNet-test	tieredImageNet-train	tieredImageNet-test
Reference	Vinyals et al. (2016)	Vinyals et al. (2016)	Ren et al. (2018)	Ren et al. (2018)
# of classes	64	20	351	160
# of samples	38,400	12,000	448,695	206,209

Datasets	CropDisease	EuroSAT	ISIC	ChestX
Reference	Mohanty et al. (2016)	Helber et al. (2019)	Codella et al. (2019)	Wang et al. (2017)
# of classes	38	10	7	7
# of samples	43,456	27,000	10,015	25,848

Datasets	Places	Plantae	Cars	CUB
Reference	Zhou et al. (2017)	Van Horn et al. (2018)	Krause et al. (2013)	Welinder et al. (2010)
# of classes	16	69	196	200
# of samples	27,440	26,650	16,185	11,788

Figure 4 shows the class distribution of each target dataset considered in our study. We observe major differences in the class distributions. For example, the EuroSAT, Places, and CUB datasets have overall balanced class distributions, while the ISIC dataset is extremely unbalanced, with the number of samples per class ranging from 115 to 9,547. We also see that the number of samples per class varies over the eight datasets. The average number of samples per class for the ChestX dataset is 3,693, while, for the CUB dataset, this number goes down to only 59.

We posit that the class distribution contributes to the difficulty of each dataset, thus implicitly considered as part of our analysis on target datasets. However, we note that class imbalance is not the deciding factor of dataset difficulty. For example, the CropDisease dataset has a relatively imbalanced class distribution, yet is shown to have very low difficulty in our study. Explicitly, the effects of class distribution on CD-FSL have not been studied in our paper.

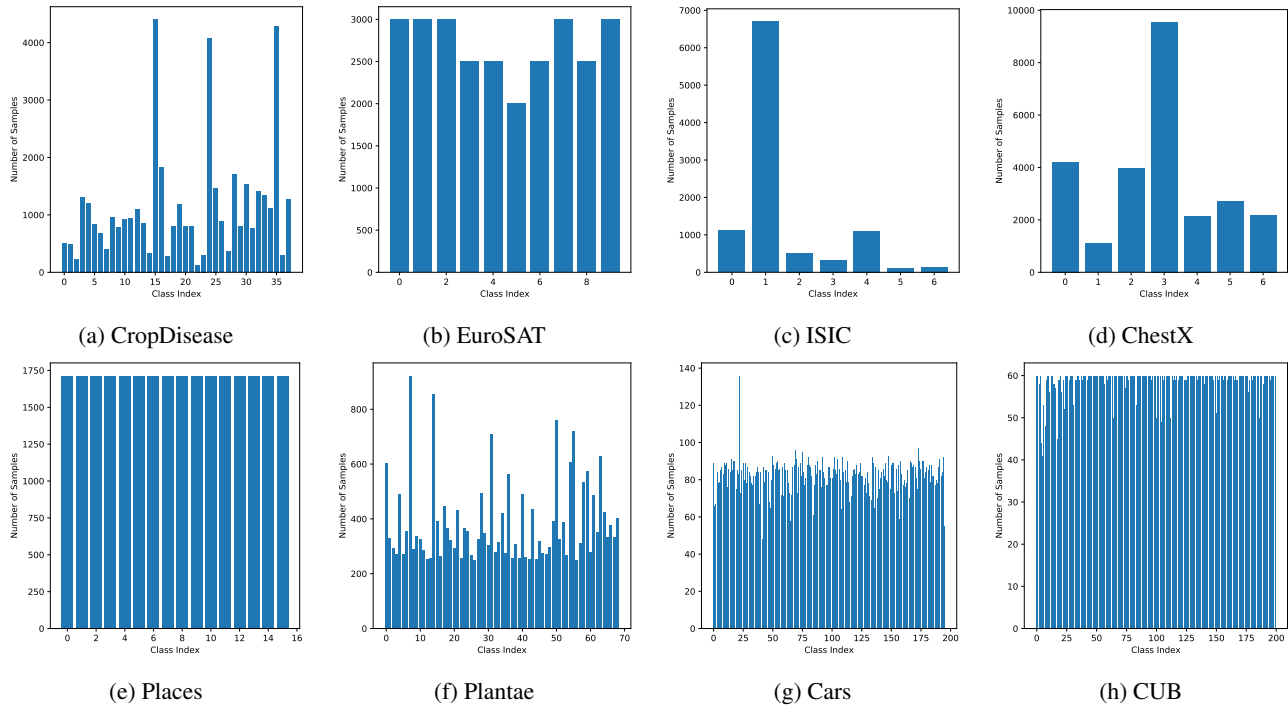


Figure 4. Class distributions of eight target datasets considered in our study.

B.2. Image Examples

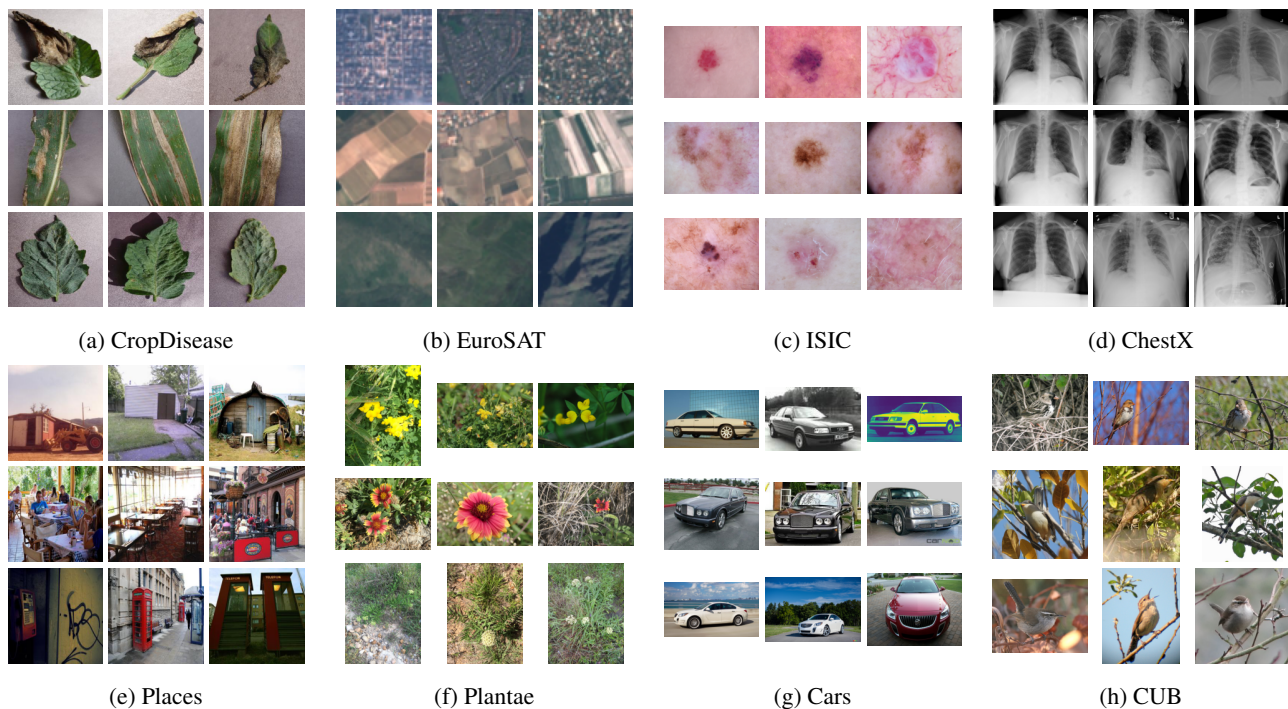


Figure 5. Image examples from eight target datasets considered in our study. Each row displays three samples from a distinct class randomly sampled from each target dataset.

We illustrate the qualitative characteristics of eight target domains for CD-FSL by showing nine randomly sampled examples from three distinct classes for each target dataset in Figure 5. The previous work (Guo et al., 2020) defined domain similarity to miniImageNet source with respect to perspective distortion, semantic contents, and color depth. This can be seen in Figure 5(a)-(d); CropDisease consists of natural images regarding agriculture, EuroSAT contains satellite images taken from a fixed perspective, ISIC and ChestX contain images with fixed perspective and unique semantics, with ChestX being grayscale. On the other hand, non-BSCD-FSL datasets in Figure 5(e)-(h) depict familiar scenes or objects to human eyes.

Using the EMD (Earth Mover’s Distance) analysis, we discovered that domain similarity is mainly determined by the semantic contents of the images. For example, we find that ChestX and ISIC, which exhibit highly distinct semantic content, have high domain similarity with all three target datasets. CropDisease and EuroSAT have relatively higher domain similarity within the BSCD-FSL benchmark, and, this can be attributed to the fact that the image subjects are from the natural image setting, albeit with fixed perspective and lack of either background or foreground. Places shows that highest domain similarity, and this can be attributed to the existence of diverse subjects from the natural image domain, similar to the source datasets.

We can also observe that each target dataset has varying levels of difficulty. For example, for ChestX, it appears challenging in to detect the small differences between the grayscale images, and nearly impossible to distinguish any prominent features between classes to the untrained eye. On the other hand, classes from CropDisease are shown to have distinct features that are easily distinguishable.

C. Implementation Details

C.1. Training Setup

We generally follow training setup used in previous works without validation dataset. The details and minor change for CD-FSL is explained as follows:

SL Pre-Training We use an SGD optimizer with initial learning rate of 0.1, momentum of 0.9, and weight decay coefficient of 10^{-4} is used. When using miniImageNet as source data, we train ResNet10 model for 1,000 epochs with batch size 64, learning rate decayed by 1/10 at epoch {400, 600, 800}. When using tieredImageNet as source data, we train ResNet18 model for 90 epochs with batch size 256. For ImageNet, the pre-trained ResNet18 model offered by an official PyTorch (Paszke et al., 2019) library is used.

SimCLR Pre-Training We follow the setting in Phoo & Hariharan (2021) except batch size, learning rate, and augmentation method; SGD optimizer with momentum 0.9 and weight decay 10^{-4} is used. 1000 epochs are trained with batch size 32. Because SimCLR (including other SSL methods) uses a multi-viewed batch, it has an effective batch size of 64 by augmentations. Learning rate starts with 0.1 and is decayed by 1/10 times at epoch {400, 600, 800}. For the SimCLR loss, two-layer projection head (i.e., Linear-ReLU-Linear) is added on top of the extractor. The projection head uses hidden dimension of 512 and output feature dimension of 128. The temperature value of NT-Xent loss (normalized temperature-scaled cross-entropy loss, Chen et al. (2020a)) is set to 1.0.

MoCo Pre-Training We use the same optimizer, epochs, and batch size as SimCLR pre-training. The projector of both query and key is one fully-connected layer with feature of dimension 128. Also, we used moving average coefficient 0.999 for the momentum encoder and the memory bank size of 1,024. Note that the original MoCo (He et al., 2020) uses very large size of a memory bank (i.e., 65,536), mainly because large number of negative samples is required in self-supervised learning of ImageNet data. However, in the case of our self-supervised learning on small-size target data, large memory bank is neither needed nor recommended. The unlabeled target data in our study do not exceed a few thousand images. Moreover, large amount of negative samples can make the contrastive task too hard to optimize for extremely fine-grained images, as we observed in ChestX FSL performances. This is the main reason why MoCo rarely surpasses SimCLR in our experiments. Also, note that the hyperparameters are mainly suited on the SimCLR model, but we did not further search or tune the hyperparameters.

BYOL Pre-Training We use a different optimizer for BYOL; Adam (Kingma & Ba, 2014) optimizer with the initial learning rate of 3×10^{-4} . The online and target projector are both composed of two-layer MLP (i.e., Linear-BatchNorm1D-ReLU-Linear) with hidden dimension of 4,096 and projection dimension of 256. The moving average coefficient for the target network is 0.99. A predictor after the online projector is also a two-layer MLP with hidden dimension of 4,096 and output prediction dimension of 256.

SimSiam Pre-Training SimSiam uses same network structure as BYOL, except there is no auxiliary target encoder and target projector. Every other training setup is the same.

MSL Pre-Training When training the MSL model, the batch size of source data is 64 and that of target data is 32, because target data are augmented twice to make positive pairs. Although we pre-trained for 1,000 epochs, one epoch corresponds to an entire sweep over the target data. The source batch is randomly sampled at every iteration, independently from the epoch. A conflicting setting is that we used an SGD optimizer for SL pre-training and Adam optimizer for BYOL pre-training. Therefore, in MSL (BYOL) pre-training, there were two choices of an optimizer. We confirmed with some experiments that SGD optimizer better works for MSL (BYOL).

Fine-Tuning We follow the setting in Guo et al. (2020); SGD optimizer with learning rate 0.01, momentum 0.9, and weight decay 0.001 is used. Only the linear classifier is trained with frozen pre-trained extractor, and 100 epochs are trained with batch size 4. Note that, for a fair comparison, we removed a projector or predictor that is additional introduced in SSL pre-training.

C.2. Data Augmentations

We provide below the PyTorch-style code for base and strong augmentation. A short description for each transform with our set parameter is as follows:

- RandomResizedCrop: Randomly crop a portion of an image and then resize it to 224x224.
- RandomColorJitter: Randomly change the brightness, contrast, and saturation, with probability 1.0.
- RandomHorizontalFlip: Randomly flip an image in a vertical axis, with probability 0.5.
- RandomGrayscale: Randomly convert image into gray-scale, with probability 0.1.
- RandomGaussianBlur: Randomly blur an image with Gaussian blur of kernel size (5,5), with probability 0.3.

```
import torchvision.transforms as transforms

def parse_transform(transform, image_size=224):
    if transform == 'RandomResizedCrop':
        return transforms.RandomResizedCrop(image_size)

    elif transform == 'RandomColorJitter':
        return transforms.RandomApply([transforms.ColorJitter(0.4,0.4,0.4,0.0)], p=1.0)

    elif transform == 'RandomGrayscale':
        return transforms.RandomGrayscale(p=0.1)

    elif transform == 'RandomGaussianBlur':
        return transforms.RandomApply([transforms.GaussianBlur(kernel_size=(5,5))], p=0.3)

    elif transform == 'Resize':
        return transforms.Resize([image_size, image_size])

    elif transform == 'Normalize':
        return transforms.Normalize(mean=[0.485,0.456,0.406],
                                    std=[0.229,0.224,0.225])

    elif transform == 'ToTensor':
        return transforms.ToTensor()

def get_composed_transform(augmentation: str, image_size=224):
    if augmentation == 'base':
        transform_list = ['RandomResizedCrop', 'RandomColorJitter',
                          'RandomHorizontalFlip', 'ToTensor', 'Normalize']

    elif augmentation == 'strong':
        transform_list = ['RandomResizedCrop', 'RandomColorJitter',
                          'RandomGrayscale', 'RandomGaussianBlur',
                          'RandomHorizontalFlip', 'ToTensor', 'Normalize']

    elif augmentation == 'none':
        transform_list = ['Resize', 'ToTensor', 'Normalize']

    transform_funcs = [parse_transform(x, image_size=image_size) for x in transform_list]
    transform = transforms.Compose(transform_funcs)
    return transform
```

D. Domain Similarity

BSCD-FSL benchmark contains four datasets with varying levels of domain similarity: CropDisease, EuroSAT, ISIC, and ChestX. These datasets are known to be distant from the source dataset, miniImageNet. Guo et al. (2020) provided the order of domain similarity for the BSCD-FSL benchmark based on three qualitative factors, perspective distortion, semantic contents, and color depth. However, our quantitative metric in Eq. (4) shows a somewhat different order of domain similarity between the four datasets in BSCD-FSL. The known similarity order for BSCD-FSL was “CropDisease > EuroSAT > ISIC > ChestX” under the assumption that a dataset has domain similar to ImageNet if it has perspective distortion (*i.e.*, CropDisease), is natural (*i.e.*, CropDisease, EuroSAT), and has RGB color depth (*i.e.*, CropDisease, EuroSAT, ISIC).

In contrast, with our quantitative metric, we observe a different order of “EuroSAT > CropDisease > ISIC \approx ChestX” in Table 5. It turns out that only the semantic content is a significant factor to decide domain similarity; thus, the two medical datasets, ISIC and ChestX, show domain similarity smaller than others. On the other hand, the perspective distortion and color depth is not significant considering that (1) the order of CropDisease and EuroSAT is reversed and (2) ISIC and ChestX show almost the same domain similarity regardless of their different color depth. Therefore, it is believed that the semantic content is the most significant factor to determine domain similarity.

Table 5. Domain Similarity. Earth mover distance (EMD) and similarity (calculated by $\exp(-\alpha \times \text{EMD})$) are reported. The used feature extractor is ResNet101 provided by PyTorch (Paszke et al., 2019). Rank 1 dataset indicates that the source and target datasets are the most similar.

		Places	CUB	Cars	Plantae	EuroSAT	CropDisease	ISIC	ChestX
EMD	IN	18.14	18.91	20.13	20.31	21.67	21.88	22.25	22.28
	tieredIN	17.26	19.90	20.23	20.63	19.20	22.07	22.94	23.19
	miniIN	17.49	19.38	20.34	20.29	21.10	21.66	22.20	22.33
Sim	IN	0.834 (1)	0.828 (2)	0.818 (3)	0.816 (4)	0.805 (5)	0.803 (6)	0.801 (7)	0.800 (8)
	tieredIN	0.841 (1)	0.820 (3)	0.817 (4)	0.814 (5)	0.825 (2)	0.802 (6)	0.795 (7)	0.793 (8)
	miniIN	0.840 (1)	0.824 (2)	0.816 (4)	0.816 (3)	0.810 (5)	0.805 (6)	0.801 (7)	0.800 (8)

E. Few-Shot Difficulty

We quantify few-shot difficulty using our empirical upper bound on each dataset following in Eq. (5). Few-shot difficulty is depends on a backbone network and k . Table 6 describes few-shot difficulty according to the combination of our backbone (ResNet10 and ResNet18) and k . It is observed that the order of few-shot difficulty for datasets are the same except for the order between ISIC and CUB when ResNet10 is used as backbone and $k=1$.

Table 6. Few-shot difficulty (ranking). 5-way k -shot performances are reported. To quantify the data difficulty, we designed the upper performance case, where we use SL pre-training with 20% of target data as labeled data. The k -shot difficulty is calculated by $\text{Diff}@k = \exp(-\beta \times \text{Perf}@k)$. Rank 1 dataset is the most difficult one.

Backbone	k	CropDisease	EuroSAT	ISIC	ChestX	Places	Plantae	Cars	CUB
RN18	1	96.92 \pm .32	90.51 \pm .55	42.83 \pm .80	31.00 \pm .60	63.97 \pm .87	52.83 \pm .89	48.71 \pm .82	42.96 \pm .76
	5	99.51 \pm .10	96.74 \pm .21	55.55 \pm .67	39.19 \pm .58	81.56 \pm .57	74.24 \pm .71	72.83 \pm .67	64.03 \pm .77
	20	99.69 \pm .07	97.45 \pm .17	61.32 \pm .62	42.11 \pm .56	86.10 \pm .47	82.17 \pm .64	82.08 \pm .53	74.14 \pm .66
	Diff@1	0.379 (8)	0.405 (7)	0.652 (2)	0.733 (1)	0.527 (6)	0.590 (5)	0.614 (4)	0.651 (3)
	Diff@5	0.370 (8)	0.380 (7)	0.574 (2)	0.676 (1)	0.442 (6)	0.476 (5)	0.483 (4)	0.527 (3)
	Diff@20	0.369 (8)	0.377 (7)	0.542 (2)	0.656 (1)	0.423 (6)	0.440 (5)	0.440 (4)	0.476 (3)
RN10	1	92.44 \pm .55	83.34 \pm .68	42.89 \pm .77	28.89 \pm .55	57.25 \pm .82	49.08 \pm .83	43.32 \pm .72	40.72 \pm .73
	5	99.00 \pm .15	95.37 \pm .26	56.94 \pm .65	36.59 \pm .56	77.39 \pm .63	70.56 \pm .76	66.40 \pm .68	60.29 \pm .78
	20	99.54 \pm .07	97.28 \pm .18	63.93 \pm .58	42.03 \pm .55	84.62 \pm .49	80.50 \pm .65	78.56 \pm .57	71.71 \pm .67
	Diff@1	0.397 (8)	0.435 (7)	0.651 (3)	0.749 (1)	0.564 (6)	0.612 (5)	0.648 (4)	0.666 (2)
	Diff@5	0.372 (8)	0.385 (7)	0.566 (2)	0.694 (1)	0.461 (6)	0.494 (5)	0.515 (4)	0.547 (3)
	Diff@20	0.370 (8)	0.378 (7)	0.528 (2)	0.657 (1)	0.429 (6)	0.447 (5)	0.456 (4)	0.488 (3)

F. Domain Similarity and Few-Shot Difficulty Visualizations

In this section, we provide visualizations of domain similarity and few-shot difficulty. Domain similarity is dependent on the source dataset, and few-shot difficulty is dependent on backbone network (*e.g.*, ResNet10 and ResNet18) and *k*. Figure 6 visualizes domain similarity and few-shot difficulty for eight datasets, as depicted in Appendix D and E. Figure 6(a,b,c) have the same domain similarity, Figure 6(d,e,f) have the same, and Figure 6(g,h,i) have the same, because domain similarity is based on the source dataset. For few-shot difficulty, Figure 6(a,d) have the same difficulty, 6(b,e) have the same, and (c,f) have the same, because few-shot difficulty is based on backbone network and *k*.

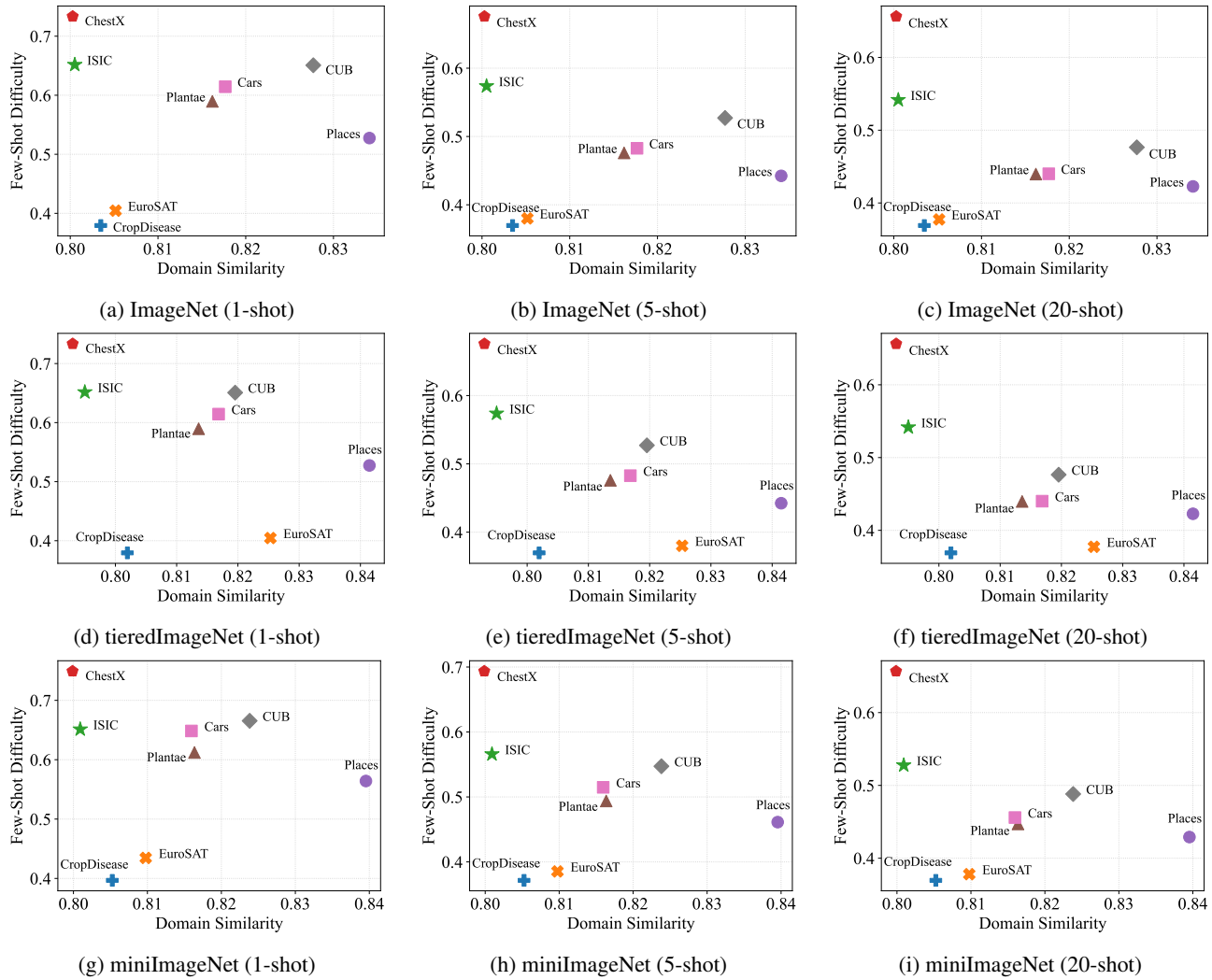


Figure 6. Domain similarity and few-shot difficulty for eight benchmark datasets.

G. Performance of SSL according to the Ratio of Unlabeled Target Data

In this section, we evaluate few-shot performance of SSL (SimCLR and BYOL) according to the ratio of unlabeled target data when ResNet10 is used as a backbone network. Figure 7 and Figure 8 describe the few-shot performance according to the ratio of unlabeled target data when SimCLR and BYOL are used for SSL method, respectively. We control the ratio $\in \{5\%, 10\%, 20\%, 40\%, 80\%\}$. We further evaluate few-shot performance of SSL (SimCLR) when ResNet18 is used as a backbone network, depicted as Figure 9.

It is observed that except for ChestX, SimCLR with a small portion (even 5%) of target data as unlabeled data has better performance than SL that uses ImageNet, tieredImageNet, and miniImageNet. Note that ImageNet and tieredImageNet include around 1.3 million and 0.45 million samples with annotations, respectively. On the other hand, 5% of EuroSAT, CropDisease, and ISIC unlabeled data include around 1.4k, 2.2k, and 0.5k samples. It implies that the consistency between source and target domains is much more important than the number of data for pre-training.

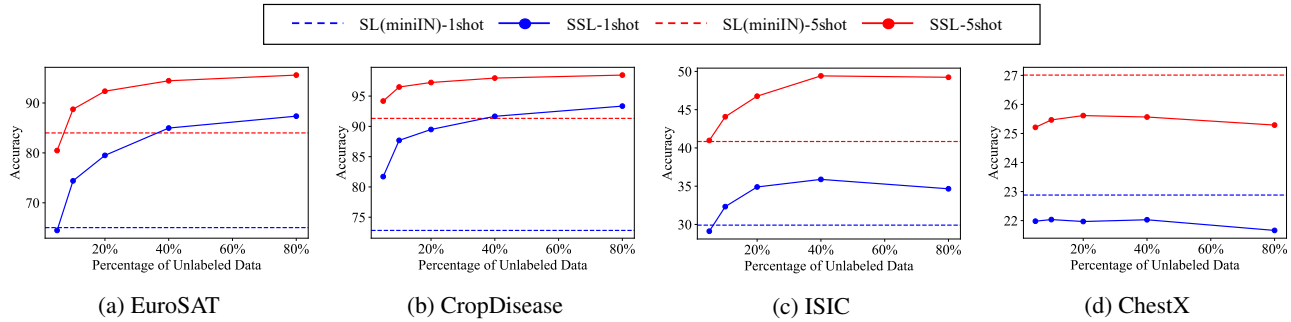


Figure 7. 5way- k shot performance of SSL (SimCLR) according to the ratio of unlabeled target data and SL (Section 4). ResNet10 is used as a backbone. Blue and red lines indicate 1-shot and 5-shot accuracy, respectively. Dotted and solid lines are accuracy of SL (miniIN) and SSL (SimCLR), respectively.

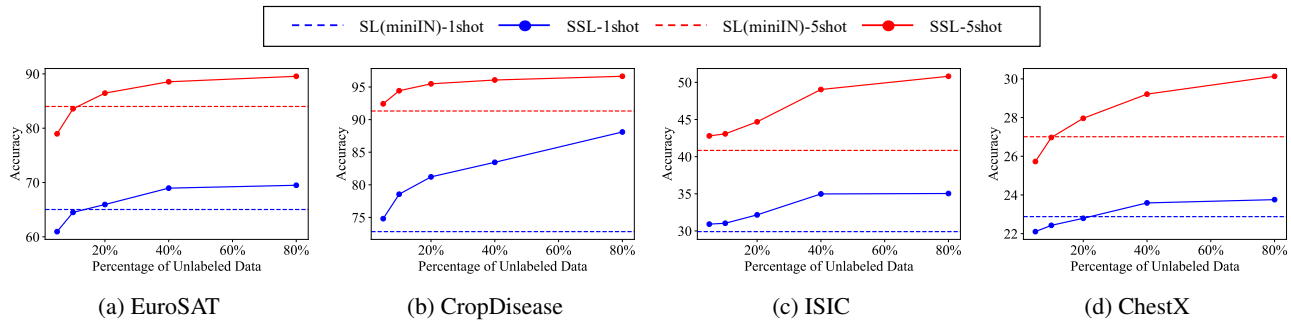


Figure 8. 5way- k shot performance of SSL (BYOL) according to the ratio of unlabeled target data and SL (Section 4). ResNet10 is used as a backbone. Blue and red lines indicate 1-shot and 5-shot accuracy, respectively. Dotted and solid lines are accuracy of SL (miniIN) and SSL (BYOL), respectively.

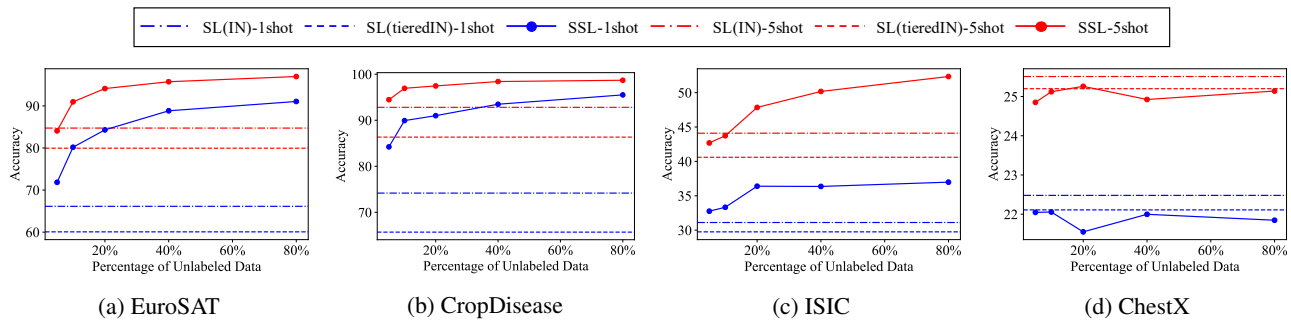


Figure 9. 5way- k shot performance of SSL according to the ratio of unlabeled target data and SL (Section 4). ResNet18 is used as a backbone. SimCLR is used for the SSL method.

H. Performance of SL and SSL for the Other Datasets

Table 7 summarizes the full performance numbers of SL and SSL on non-BSCD-FSL datasets, of which some results were provided in Figure 2(a) and Figure 2(b) in main paper. We would like to highlight that unlike BSCD-FSL sets, these 4 target domains take a big advantage from the ImageNet domain. SL (IN) results indicate comparable or even better (in Cars and CUB) results than SSL. We elaborate the details for the ImageNet-source SL model in Appendix K.

Table 7. 5way- k shot CD-FSL performance of the models pre-trained by SL and SSL, on four additional target datasets: Places, Plantae, Cars, and CUB. We report the average accuracy and its 95% confidence interval over 600 few-shot episodes. B and S indicate base and strong augmentations, respectively. The best results are marked in bold and the second best are underlined. We include the result when using the model pre-trained on the entire ImageNet data, which also uses the ResNet18 backbone as tieredImageNet experiments.

Source Data	Pre-train Scheme	Method	Aug.	Places		Plantae		Cars		CUB			
				$k=1$	$k=5$	$k=1$	$k=5$	$k=1$	$k=5$	$k=1$	$k=5$		
ImageNet	SL	Default	B	<u>57.47</u> \pm .86	<u>79.22</u> \pm .64	<u>43.66</u> \pm .80	63.21 \pm .82	45.82 \pm .79	66.38 \pm .80	65.24 \pm .97	83.93 \pm .66		
tieredImageNet	SL	Default	B	52.07 \pm .86	72.12 \pm .69	38.63 \pm .74	54.76 \pm .82	31.23 \pm .65	42.59 \pm .70	<u>57.94</u> \pm .93	<u>76.86</u> \pm .78		
			S	52.82 \pm .86	72.96 \pm .67	34.99 \pm .64	51.11 \pm .76	31.05 \pm .63	42.32 \pm .69	54.18 \pm .91	74.14 \pm .80		
-	SSL	SimCLR	B	45.82 \pm .85	62.07 \pm .78	38.52 \pm .74	53.89 \pm .80	28.86 \pm .68	37.05 \pm .69	33.56 \pm .67	43.99 \pm .71		
			S	64.97 \pm .94	80.43 \pm .61	44.18 \pm .85	60.07 \pm .84	32.46 \pm .70	44.55 \pm .74	36.15 \pm .76	47.36 \pm .79		
		MoCo	B	39.64 \pm .82	53.95 \pm .77	35.17 \pm .73	48.83 \pm .76	27.40 \pm .64	34.59 \pm .67	29.67 \pm .59	36.93 \pm .61		
			S	55.53 \pm .74	71.50 \pm .73	36.49 \pm .73	49.15 \pm .76	29.36 \pm .67	38.44 \pm .70	31.76 \pm .66	40.81 \pm .72		
		BYOL	B	40.38 \pm .72	60.06 \pm .73	38.60 \pm .72	57.81 \pm .81	31.04 \pm .66	41.79 \pm .72	35.27 \pm .67	49.61 \pm .71		
			S	51.76 \pm .79	72.47 \pm .63	42.16 \pm .75	<u>61.02</u> \pm .82	<u>34.54</u> \pm .70	<u>48.56</u> \pm .76	36.50 \pm .68	51.31 \pm .78		
		SimSiam	B	35.27 \pm .68	48.12 \pm .69	36.11 \pm .76	48.63 \pm .79	28.30 \pm .64	35.24 \pm .65	29.96 \pm .62	37.61 \pm .60		
			S	52.56 \pm .92	68.29 \pm .74	36.19 \pm .69	50.23 \pm .76	31.21 \pm .64	43.06 \pm .67	33.73 \pm .71	43.22 \pm .74		
		(a) ResNet18 is used as a backbone.											
		mini ImageNet	SL	Default	B	51.84 \pm .80	72.19 \pm .70	37.28 \pm .69	54.15 \pm .74	30.79 \pm .56	44.36 \pm .69	40.65 \pm .78	58.54 \pm .81
S	<u>52.45</u> \pm .78				<u>72.92</u> \pm .66	36.72 \pm .67	53.26 \pm .73	30.20 \pm .54	<u>44.39</u> \pm .66	<u>40.56</u> \pm .78	<u>58.10</u> \pm .78		
-	SSL	SimCLR	B	44.06 \pm .78	62.86 \pm .78	38.43 \pm .77	54.68 \pm .80	28.59 \pm .66	38.24 \pm .73	33.88 \pm .68	45.31 \pm .73		
			S	58.75 \pm .93	78.39 \pm .61	42.65 \pm .80	59.77 \pm .82	<u>30.89</u> \pm .66	45.60 \pm .72	35.49 \pm .73	47.69 \pm .77		
		MoCo	B	38.41 \pm .74	54.65 \pm .74	33.96 \pm .69	47.51 \pm .72	28.03 \pm .66	36.19 \pm .72	32.37 \pm .65	40.55 \pm .72		
			S	52.05 \pm .90	71.57 \pm .70	36.36 \pm .73	50.37 \pm .78	28.25 \pm .61	38.89 \pm .69	33.53 \pm .72	42.87 \pm .74		
		BYOL	B	40.60 \pm .69	59.28 \pm .71	<u>39.27</u> \pm .73	<u>55.87</u> \pm .79	30.11 \pm .62	41.21 \pm .69	34.74 \pm .65	49.10 \pm .74		
			S	47.81 \pm .75	68.14 \pm .68	39.12 \pm .71	55.31 \pm .79	31.53 \pm .65	43.92 \pm .70	35.96 \pm .70	49.34 \pm .76		
		SimSiam	B	39.27 \pm .72	53.40 \pm .74	37.12 \pm .72	50.61 \pm .81	28.49 \pm .62	35.50 \pm .67	30.37 \pm .63	38.22 \pm .62		
			S	51.62 \pm .81	69.77 \pm .66	38.49 \pm .73	53.10 \pm .78	30.00 \pm .59	40.92 \pm .67	34.25 \pm .71	44.85 \pm .74		
		(b) ResNet10 is used as a backbone.											

I. Analyses on Other Source Datasets

In this section, we expand our analyses of SL and SSL on ImageNet source in Section 5, onto two additional source datasets: tieredImageNet and miniImageNet. Every observation that was previously identified on ImageNet is consistently made in the two additional source datasets.

I.1. Limitations of Domain Similarity (Observation 5.1)

Figure 10 shows the performance of SL and SSL for three source datasets and eight target datasets, according to domain similarity. Across all source datasets, we consistently find that domain similarity alone is not sufficient to explain the relative performance of SL, compared to SSL. As mentioned in Section 5, we observe that SSL can outperform SL even when domain similarity is large, as highlighted by the difference between Places and CUB shown in Figures 10(a,b) for ImageNet, which are identical to Figures 2(a,b) in the main paper. Similar observations are made between EuroSAT and CUB for tieredImageNet in Figures 10(c,d), and between Places and CUB for miniImageNet in Figures 10(e,f).

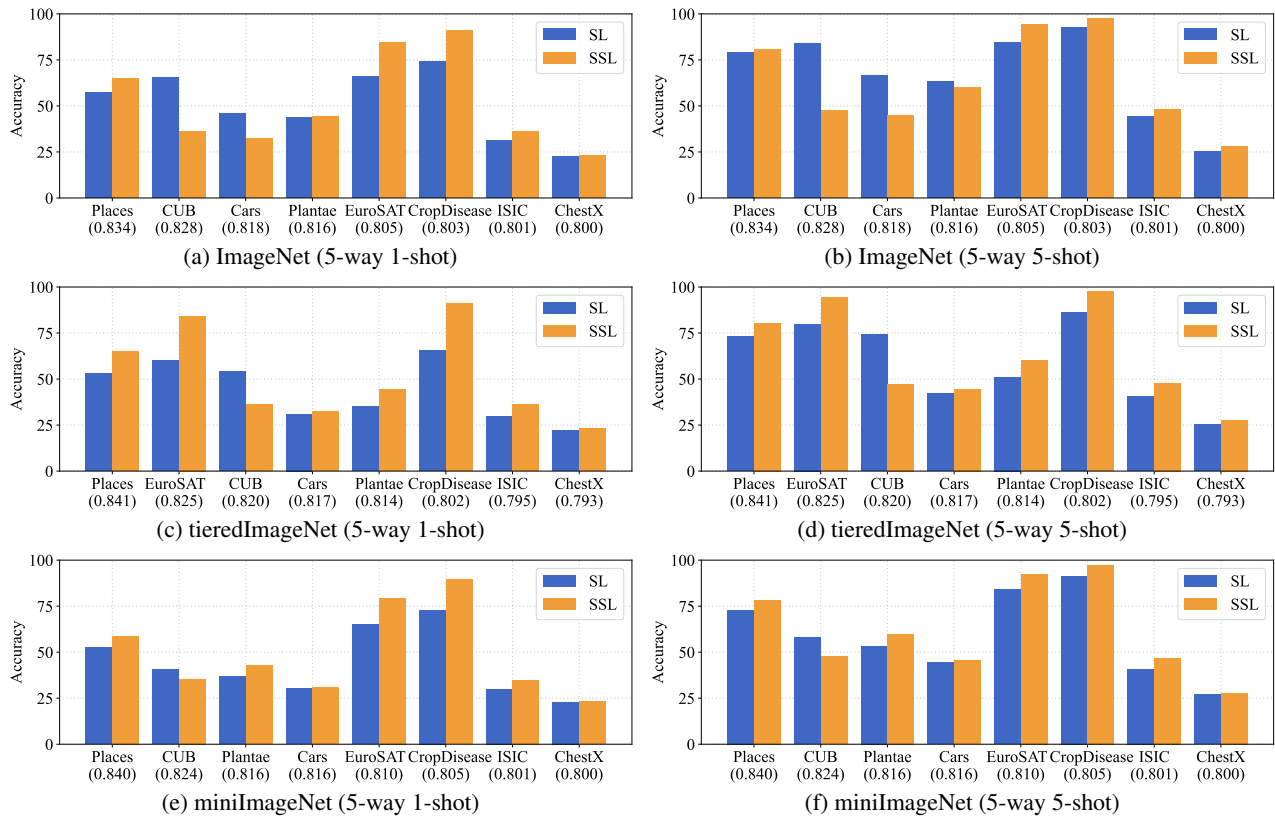


Figure 10. 5-way k -shot CD-FSL performance (%) of SL and SSL according to domain similarity. Target datasets are shown in order of domain similarity (values in x-axis) to ImageNet, tieredImageNet and miniImageNet, respectively. For SSL, SimCLR is used for all datasets except ChestX, for which BYOL is used.

I.2. When Does Performance Gain of SSL over SL Become Greater? (Observation 5.2)

Figure 11 shows the performance gain of SSL over SL for three source datasets and eight target datasets, according to few-shot difficulty, for two groups with different levels of domain similarity. Again, the identical observation is made for all three source datasets. When comparing the two groups (BSCD-FSL vs. others), larger performance gain is observed for the small domain similarity group (BSCD-FSL), compared to the latter (others). Within each group, the performance gain of SSL over SL increases with lower few-shot difficulty.

In addition, comparing between different source datasets, for target datasets with large similarity (Figure 11(b,d,f)), the performance gain of SSL over SL decreases by larger source dataset size. For example, on the CUB dataset, the performance gain (for $k = 5$) is -0.249 , -1.035 , and -2.276 for miniImageNet, tieredImageNet, and ImageNet, respectively. However, for target datasets with small similarity (Figure 11(a,c,e)), the performance gain of SSL over SL does not have a consistent trend according to the source dataset size.

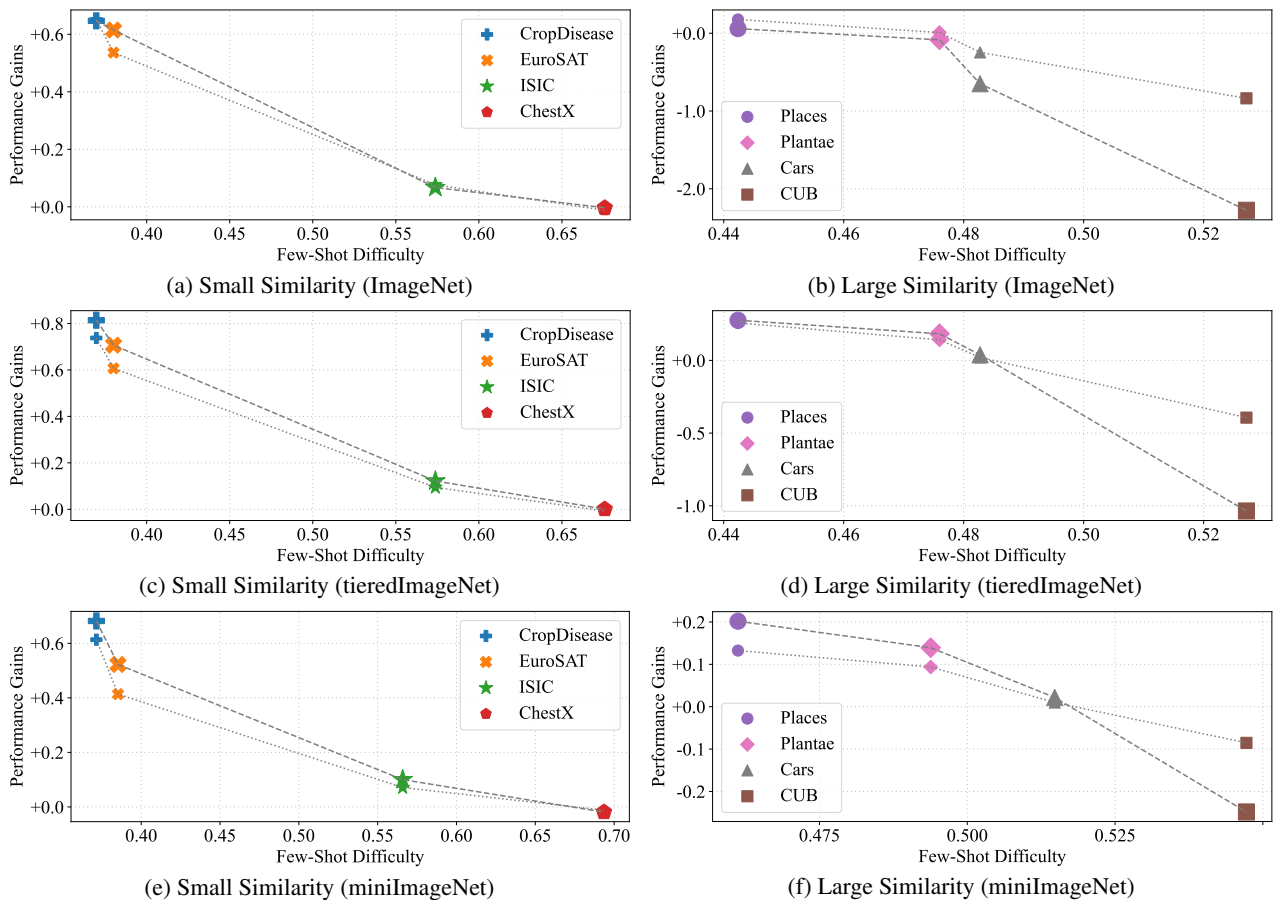


Figure 11. 5-way k -shot performance gains of SSL over SL for the two dataset groups according to the few-shot difficulty (small: $k=1$, large: $k=5$). Results are shown for three source datasets: ImageNet, tieredImageNet, and miniImageNet, each with their corresponding backbones. SimCLR used for SSL in all target datasets except ChestX, for which BYOL is used. Figures 11(a,b) show results identical to those from Figure 3 and is added for convenience.

J. Hyperparameter γ in MSL Pre-Training

One important hyperparameter in MSL is a balancing weight γ (refer to Eq. (3)). We investigated how we should choose γ value. Figure 12 and Figure 13 describe the few-shot performance of MSL according to the balancing weight γ between SL and SSL when SimCLR or BYOL are used for SSL, respectively. In Figure 12, MSL performance (circle-marked solid lines) generally improves as γ increases from 0.125 to 0.875, i.e., the weight for SSL is getting larger, except for ChestX. In Section 4, we found that non-contrastive SSL method nicely worked on ChestX. Figure 13 shows that MSL with BYOL loss guarantees good performance on ChestX in $\gamma = 0.875$. We further increased γ to $\{0.9, 0.95, 0.99\}$, but there was an overall decreasing trend of accuracy, so we fixed γ to 0.875 in every MSL experiment in the paper.

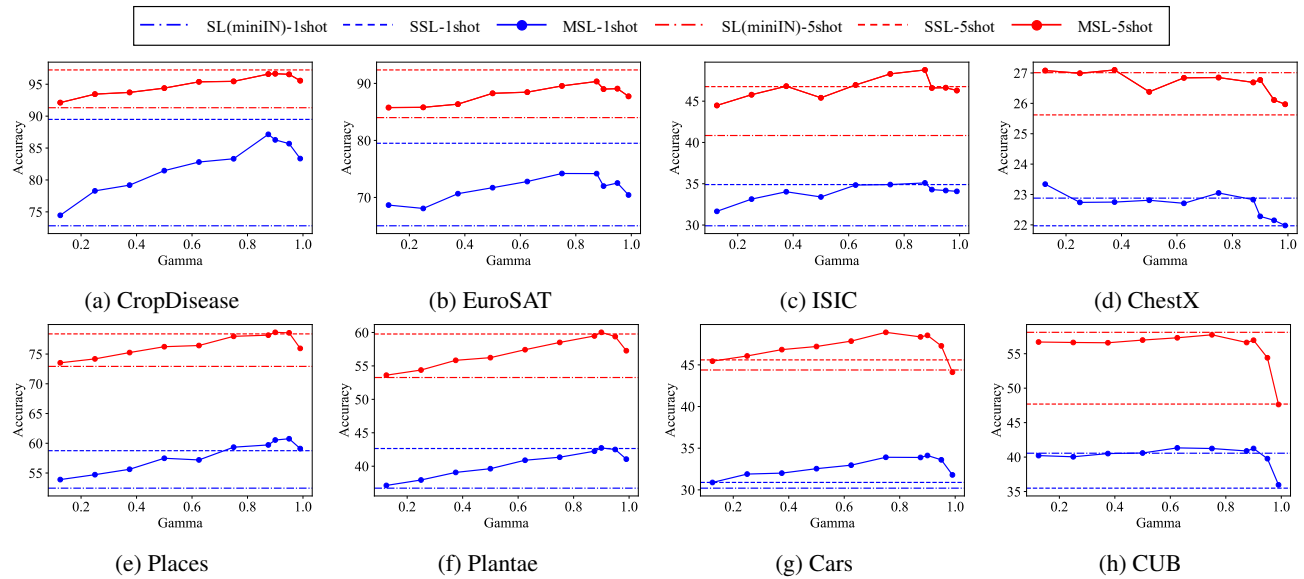


Figure 12. 5-way k -shot performance of MSL according to the balancing weight (i.e., γ) between SL and SSL (Section 6). ResNet10 is used as a backbone. SimCLR is used for the MSL and SSL method.

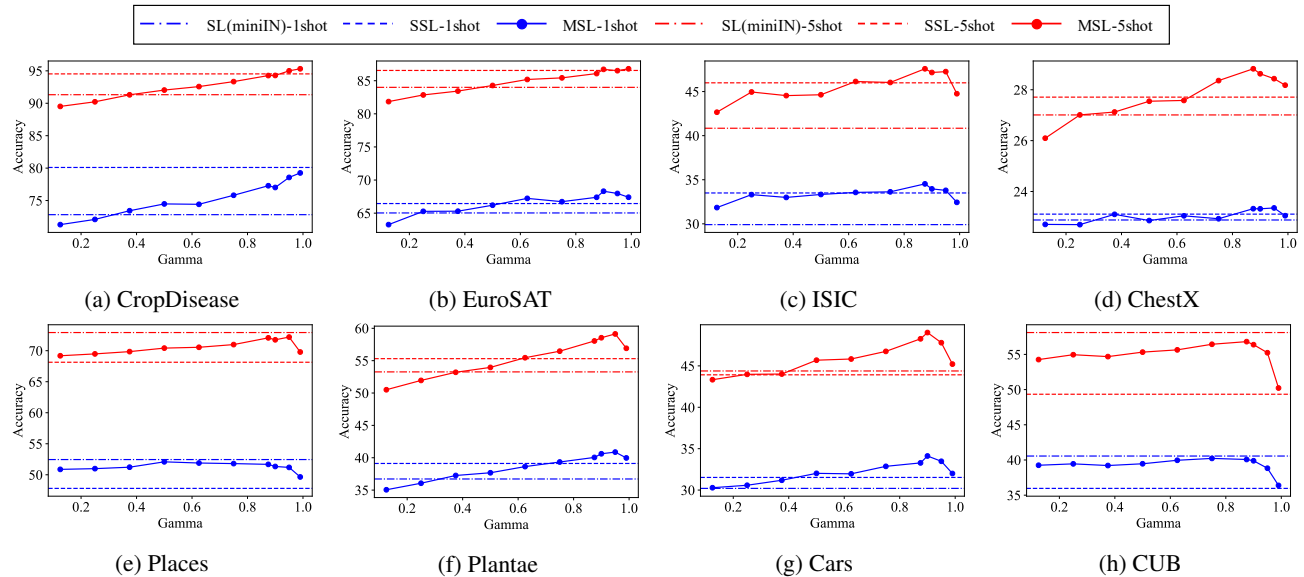


Figure 13. 5-way k -shot performance of MSL according to the balancing weight (i.e., γ) between SL and SSL (Section 6). ResNet10 is used as a backbone. BYOL is used for the MSL and SSL method.

K. Increasing Batch Size on the Source Dataset for MSL

Obviously, the total size of labeled source dataset and that of unlabeled target dataset are significantly different. For example, ImageNet has around 1.3M examples, however, Cars and CUB has around 3,400 and 2,350 examples when 20% of data is used as unlabeled data, respectively. Therefore, even if 1,000 epochs are executed on unlabeled target data, only 2-3 epochs on ImageNet (refer to **MSL Pre-Training** setup in Appendix C.1). In particular, we have found that when domain similarity is large, SL is important. To remedy this problem, we only increase batch size for the source data, keeping the batch size for the target data fixed to 64.

Table 8 describes CD-FSL performance according to the source batch size on Cars and CUB. It is shown that larger batch size for the source dataset can improve the MSL performance. We suppose that the MSL model with ImageNet obtains large generalization ability from large-scale data, gaining much larger benefit than miniImageNet or tieredImageNet source. This improvement is significant in Cars and CUB datasets because they are similar to ImageNet. In fact, ImageNet data already includes car types (~ 10 classes) and bird species (~ 59 classes).

Table 8. 5-way k -shot performance of MSL according to the source batch size when ImageNet is used as source.

Target Dataset	Method	Batch Size for Source Dataset	$k=1$	$k=5$
Cars	SimCLR	64 (default)	36.96 \pm .77	51.84 \pm .79
		128	38.54 \pm .81	53.80 \pm .84
		256	38.24 \pm .78	54.18 \pm .81
		512	38.98 \pm .81	55.25 \pm .81
	BYOL	64 (default)	33.31 \pm .66	46.76 \pm .73
		128	39.85 \pm .81	58.01 \pm .80
		256	41.45 \pm .82	59.48 \pm .80
		512	40.98 \pm .80	59.48 \pm .81
CUB	SimCLR	64 (default)	47.35 \pm .87	64.53 \pm .80
		128	49.91 \pm .87	68.01 \pm .81
		256	51.06 \pm .85	69.51 \pm .79
		512	51.48 \pm .88	70.13 \pm .79
	BYOL	64 (default)	50.71 \pm .87	69.67 \pm .82
		128	52.75 \pm .87	72.26 \pm .79
		256	54.17 \pm .86	73.50 \pm .79
		512	53.70 \pm .86	73.31 \pm .80

L. Results Summary

L.1. Source Dataset: ImageNet

Table 9 and Table 10 describe 5-way 1-shot and 5-way 5-shot CD-FSL performance when ImageNet is used as the source dataset, respectively. Note that Table 10 is added for convenience and this is the same with Table 3 in the main paper. The results of STARTUP and DynDistill are from Phoo & Hariharan (2021) and Islam et al. (2021a), respectively.

Table 9. 5-way 1-shot CD-FSL performance (%) of the models pre-trained by SL, SSL, and MSL including their two-stage versions. ResNet18 is used as the backbone model, and ImageNet is used as the source data for SL. The balancing coefficient γ in Eq. (3) of MSL is set to be 0.875. The best results are marked in bold and the second best are underlined.

	Pre-train Scheme	Method	Small Similarity				Large Similarity			
			CropDisease	EuroSAT	ISIC	ChestX	Places	Plantae	Cars	CUB
Single-Stage	SL	Default	74.18±.82	66.14±.83	31.11±.55	22.48±.39	57.47±.86	43.66±.80	45.82±.79	65.24±.97
	SSL	SimCLR	91.00±.76	84.30±.73	36.39±.66	21.55±.41	64.97±.94	44.18±.85	32.46±.70	36.15±.76
		BYOL	85.77±.73	66.16±.86	34.53±.62	<u>22.75±.41</u>	51.76±.79	42.16±.75	34.54±.70	36.50±.68
MSL	SimCLR	88.38±.70	73.97±.79	34.02±.62	22.04±.40	65.13±.88	47.47±.86	36.96±.77	47.35±.87	
	BYOL	86.47±.74	73.18±.83	37.10±.67	23.97±.44	61.40±.87	48.31±.86	33.31±.66	<u>50.71±.87</u>	

(a) Performance comparison for single-stage schemes.

Two-Stage	SL→SSL	SimCLR	92.24±.70	86.51±.67	36.11±.67	21.75±.41	71.05±.92	49.02±.91	37.43±.79	42.40±.85
		BYOL	87.64±.70	74.05±.84	35.62±.65	23.01±.43	58.12±.87	48.28±.88	38.23±.75	42.48±.82
	SL→MSL	SimCLR	91.46±.66	77.62±.76	34.46±.64	22.50±.41	69.50±.87	51.27±.91	40.39±.82	62.12±.93
BYOL		88.37±.73	71.54±.78	<u>36.08±.63</u>	24.42±.45	63.40±.86	53.65±.88	46.62±.85	64.33±.93	
SL→MSL+	STARTUP	85.10±.74	73.83±.77	31.69±.59	<u>23.03±.42</u>	-	-	-	-	
	DynDistill	-	-	-	-	-	-	-	-	

(b) Performance comparison for two-stage schemes.

Table 10. 5-way 5-shot CD-FSL performance (%) of the models pre-trained by SL, SSL, and MSL including their two-stage versions. ResNet18 is used as the backbone model, and ImageNet is used as the source data for SL. The balancing coefficient γ in Eq. (3) of MSL is set to be 0.875. The best results are marked in bold and the second best are underlined.

	Pre-train Scheme	Method	Small Similarity				Large Similarity			
			CropDisease	EuroSAT	ISIC	ChestX	Places	Plantae	Cars	CUB
Single-Stage	SL	Default	92.81±.45	84.73±.51	44.10±.58	25.51±.44	79.22±.64	63.21±.82	66.38±.80	83.93±.66
	SSL	SimCLR	97.46±.34	94.12±.32	47.85±.65	25.26±.44	80.43±.61	60.07±.84	44.55±.74	47.36±.79
		BYOL	<u>96.93±.30</u>	87.83±.48	47.59±.63	<u>28.36±.46</u>	72.47±.63	61.02±.82	48.56±.76	51.31±.78
MSL	SimCLR	96.50±.35	90.11±.40	45.38±.63	26.05±.44	82.56±.58	64.76±.83	51.84±.79	64.53±.80	
	BYOL	96.74±.31	<u>90.82±.40</u>	49.14±.70	29.58±.47	<u>81.27±.59</u>	67.39±.81	46.76±.73	<u>69.67±.82</u>	

(a) Performance comparison for single-stage schemes.

Two-Stage	SL→SSL	SimCLR	97.88±.30	95.28±.27	48.38±.60	25.25±.44	84.40±.53	66.35±.82	51.31±.84	57.11±.88
		BYOL	<u>97.58±.26</u>	91.82±.39	<u>49.32±.63</u>	<u>28.27±.48</u>	78.87±.60	67.83±.82	54.70±.84	60.60±.82
	SL→MSL	SimCLR	97.49±.30	91.70±.35	47.43±.62	26.24±.44	85.76±.52	69.24±.81	58.97±.82	81.51±.72
BYOL		97.09±.31	90.89±.40	50.72±.67	30.20±.48	83.29±.55	74.16±.77	68.87±.80	84.34±.67	
SL→MSL+	STARTUP	96.06±.33	89.70±.41	46.02±.59	27.24±.46	-	-	-	-	
	DynDistill	-	-	-	-	-	-	-	-	

(b) Performance comparison for two-stage schemes.

L.2. Source Dataset: tieredImageNet

Table 11 and Table 12 describe 5-way 1-shot and 5-way 5-shot CD-FSL performance when tieredImageNet is used as the source dataset, respectively. Note that Dynamic Distillation (Islam et al., 2021a) used a larger ResNet-18 backbone model than our setting, which is provided by Tian et al. (2020b). The difference of the result of tieredImageNet from the result of ImageNet as the source dataset is that one-stage MSL can outperform SL on Cars and CUB datasets. It is considered that bigger source dataset makes SL stronger, as we have addressed this issue in Appendix I.

Table 11. 5-way 1-shot CD-FSL performance (%) of the models pre-trained by SL, SSL, and MSL including their two-stage versions. ResNet18 is used as the backbone model, and tieredImageNet is used as the source data for SL. The balancing coefficient γ in Eq. (3) of MSL is set to be 0.875. The best results are marked in bold and the second best are underlined.

	Pre-train Scheme	Method	Small Similarity				Large Similarity			
			CropDisease	EuroSAT	ISIC	ChestX	Places	Plantae	Cars	CUB
Single-Stage	SL	Default	65.70±.94	60.07±.88	29.75±.56	22.11±.42	52.82±.86	34.99±.64	31.38±.61	<u>54.18±.91</u>
		SSL	91.00±.76	84.30±.73	<u>36.39±.66</u>	21.55±.41	64.97±.94	44.18±.85	32.46±.70	36.15±.76
	BYOL	SSL	85.77±.73	66.16±.86	34.53±.62	<u>22.75±.41</u>	51.76±.79	42.16±.75	34.54±.70	36.50±.68
		MSL	87.44±.72	<u>77.42±.77</u>	35.47±.64	21.95±.40	<u>63.83±.93</u>	<u>46.47±.87</u>	34.65±.74	50.41±.90
	BYOL	MSL	84.67±.78	68.45±.81	37.30±.66	24.41±.44	60.07±.87	46.49±.83	37.88±.75	54.43±.88

(a) Performance comparison for single-stage schemes.

Two-Stage	SL→SSL	SimCLR	92.41±.70	86.61±.66	36.95±.67	21.75±.40	68.51±.94	47.92±.88	35.37±.77	44.74±.86
		BYOL	84.82±.76	66.92±.84	<u>37.19±.66</u>	<u>24.23±.46</u>	44.34±.79	44.32±.81	<u>38.49±.78</u>	44.40±.83
	SL→MSL	SimCLR	<u>90.13±.69</u>	<u>80.20±.78</u>	35.32±.64	22.18±.38	<u>64.85±.92</u>	<u>48.00±.86</u>	35.83±.75	60.87±.90
		BYOL	85.72±.76	53.92±.94	39.41±.68	24.31±.45	59.16±.86	48.48±.83	41.02±.78	61.98±.88
	SL→MSL ⁺	STARTUP	-	-	-	-	-	-	-	-
		DynDistill	84.41±.75	72.15±.75	33.87±.56	22.70±.42	-	-	-	-

(b) Performance comparison for two-stage schemes.

Table 12. 5-way 5-shot CD-FSL performance (%) of the models pre-trained by SL, SSL, and MSL including their two-stage versions. ResNet18 is used as the backbone model, and tieredImageNet is used as the source data for SL. The balancing coefficient γ in Eq. (3) of MSL is set to be 0.875. The best results are marked in bold and the second best are underlined.

	Pre-train Scheme	Method	Small Similarity				Large Similarity			
			CropDisease	EuroSAT	ISIC	ChestX	Places	Plantae	Cars	CUB
Single-Stage	SL	Default	86.34±.60	79.95±.66	40.60±.58	25.20±.41	72.96±.67	51.11±.76	45.18±.68	74.14±.80
		SSL	97.46±.34	94.12±.32	<u>47.85±.65</u>	25.26±.44	<u>80.43±.61</u>	60.07±.84	44.55±.74	47.36±.79
	BYOL	SSL	<u>96.93±.30</u>	87.83±.48	47.59±.63	<u>28.36±.46</u>	72.47±.63	61.02±.82	48.56±.76	51.31±.78
		MSL	96.68±.33	<u>91.72±.37</u>	47.55±.67	26.10±.45	81.67±.58	<u>63.96±.82</u>	48.81±.77	68.78±.82
	BYOL	MSL	96.41±.33	89.51±.42	50.95±.69	30.04±.47	80.16±.60	67.09±.80	54.75±.80	<u>73.03±.82</u>

(a) Performance comparison for single-stage schemes.

Two-Stage	SL→SSL	SimCLR	97.88±.31	95.39±.26	50.28±.61	25.31±.44	83.51±.56	65.40±.82	48.91±.83	61.80±.84
		BYOL	96.25±.31	89.39±.45	<u>53.00±.64</u>	<u>30.66±.48</u>	71.57±.63	63.06±.79	<u>55.04±.82</u>	62.78±.80
	SL→MSL	SimCLR	<u>97.43±.31</u>	<u>93.09±.33</u>	49.66±.63	26.27±.44	<u>83.03±.56</u>	<u>65.78±.85</u>	52.22±.81	<u>80.37±.76</u>
		BYOL	96.64±.32	85.97±.50	53.67±.68	30.84±.51	80.76±.56	69.77±.79	62.09±.78	82.77±.69
	SL→MSL ⁺	STARTUP	-	-	-	-	-	-	-	-
		DynDistill	95.90±.34	89.44±.42	47.21±.56	27.67±.46	-	-	-	-

(b) Performance comparison for two-stage schemes.

L.3. Source Dataset: miniImageNet

Table 13 and Table 14 describe 5-way 1-shot and 5-way 5-shot CD-FSL performance when miniImageNet is used as the source dataset, respectively. Similar to the results when tieredImageNet is used as the source dataset, one-stage MSL can outperform SL on Cars and CUB datasets.

Table 13. 5-way 1-shot CD-FSL performance (%) of the models pre-trained by SL, SSL, and MSL including their two-stage versions. ResNet10 is used as the backbone model, and miniImageNet is used as the source data for SL. The balancing coefficient γ in Eq. (3) of MSL is set to be 0.875. The best results are marked in bold and the second best are underlined.

	Pre-train Scheme	Method	Small Similarity				Large Similarity			
			CropDisease	EuroSAT	ISIC	ChestX	Places	Plantae	Cars	CUB
Single-Stage	SL	Default	72.82±.87	65.03±.88	29.91±.54	22.88±.42	52.45±.78	36.72±.67	30.20±.54	40.56±.78
		SSL	89.49 ±.74	79.50 ±.78	34.90±.64	21.97±.41	<u>58.75</u> ±.93	<u>42.65</u> ±.80	30.89±.66	35.49±.73
	MSL	SimCLR	87.15±.75	74.18±.80	35.10±.64	22.83±.41	59.72 ±.89	42.24±.80	33.89±.66	40.89±.79
		BYOL	80.10±.76	66.45±.80	33.50±.59	<u>23.11</u> ±.42	47.81±.75	39.12±.71	31.53±.65	35.96±.70
	MSL	SimCLR	87.15±.75	74.18±.80	35.10±.64	22.83±.41	59.72 ±.89	42.24±.80	33.89±.66	40.89±.79
		BYOL	74.16±.82	66.64±.81	35.63 ±.66	24.07 ±.47	53.60±.82	43.94 ±.79	35.71 ±.68	42.73 ±.78

(a) Performance comparison for single-stage schemes.

Two-Stage	SL→SSL	SimCLR	89.39 ±.82	82.64 ±.73	35.09±.64	22.15±.40	63.19 ±.92	46.30 ±.85	34.85±.74	39.92±.79
		BYOL	82.61±.76	67.67±.77	35.92 ±.68	<u>23.76</u> ±.45	53.72±.79	<u>45.02</u> ±.79	<u>37.40</u> ±.74	41.61±.75
	SL→MSL	SimCLR	<u>86.18</u> ±.77	<u>74.06</u> ±.85	33.91±.65	22.13±.40	<u>61.56</u> ±.86	43.47±.79	35.78±.72	<u>43.50</u> ±.82
		BYOL	75.77±.82	65.67±.83	<u>35.23</u> ±.66	24.47 ±.44	54.86±.81	44.68±.78	38.20 ±.71	45.82 ±.79
	SL→MSL ⁺	STARTUP	75.93±.80	63.88±.84	32.66±.60	23.09±.43	-	-	-	-
		DynDistill	82.14±.78	73.14±.84	34.66±.58	23.38±.43	-	-	-	-

(b) Performance comparison for two-stage schemes.

Table 14. 5-way 5-shot CD-FSL performance (%) of the models pre-trained by SL, SSL, and MSL including their two-stage versions. ResNet10 is used as the backbone model, and miniImageNet is used as the source data for SL. The balancing coefficient γ in Eq. (3) of MSL is set to be 0.875. The best results are marked in bold and the second best are underlined.

	Pre-train Scheme	Method	Small Similarity				Large Similarity			
			CropDisease	EuroSAT	ISIC	ChestX	Places	Plantae	Cars	CUB
Single-Stage	SL	Default	91.32±.49	84.00±.56	40.84±.56	27.01±.44	72.92±.66	53.26±.73	44.39±.66	<u>58.10</u> ±.78
		SSL	97.24 ±.33	92.36 ±.37	46.76±.61	25.62±.43	78.39 ±.61	<u>59.77</u> ±.82	45.60±.72	47.69±.77
	MSL	SimCLR	<u>96.59</u> ±.35	<u>90.34</u> ±.34	48.78 ±.62	26.69±.44	<u>78.17</u> ±.61	59.48±.82	48.36±.75	56.63±.78
		BYOL	93.71±.41	87.21±.48	<u>48.63</u> ±.66	29.86 ±.47	75.16±.64	63.45 ±.81	53.33 ±.76	60.66 ±.77

(a) Performance comparison for single-stage schemes.

Two-Stage	SL→SSL	SimCLR	96.84 ±.40	94.51 ±.32	48.23±.59	24.59±.42	81.52 ±.56	64.37±.81	50.72±.80	55.06±.84
		BYOL	95.87±.35	90.01±.43	50.33 ±.67	<u>29.94</u> ±.48	75.83±.62	<u>64.93</u> ±.79	<u>55.46</u> ±.79	59.78±.81
	SL→MSL	SimCLR	<u>96.67</u> ±.33	<u>90.18</u> ±.42	47.24±.63	26.47±.44	<u>79.95</u> ±.61	61.34±.80	52.74±.79	<u>61.33</u> ±.80
		BYOL	94.50±.39	87.96±.48	49.36±.66	30.23 ±.50	76.67±.63	65.41 ±.78	58.62 ±.78	66.20 ±.78
	SL→MSL ⁺	STARTUP	93.02±.45	82.29±.60	47.22±.61	26.94±.44	-	-	-	-
		DynDistill	95.54±.38	89.07±.47	<u>49.36</u> ±.59	28.31±.46	-	-	-	-

(b) Performance comparison for two-stage schemes.

M. Same Domain FSL Experiments

For the same domain FSL, although label space of the source and target datasets is still not shared, it is expected that SL is a better strategy and MSL improves the few-shot performance because MSL works like multi-task learning (MTL), improving the generalization ability. This is because the source and target datasets were collected in the same way.

To explain same-domain FSL experiments based on *domain similarity* and *few-shot difficulty*, we first provide them for the two datasets:

- Domain Similarity
 - miniImageNet ↔ miniImageNet-test: 0.832
 - tieredImageNet ↔ tieredImageNet-test: 0.869
- Few-shot Difficulty ($k = 5$)
 - miniImageNet-test: 0.467
 - tieredImageNet-test: 0.414

Interestingly, domain similarity of the miniImageNet-test dataset (0.832) is larger than that of every other benchmark, except for the Places (0.840). The Places dataset is found to be most similar to miniImageNet source. For the tieredImageNet-test dataset, domain similarity with tieredImageNet source (0.869) is larger than that of every other benchmark. Few-shot difficulty of miniImageNet-test is 0.467, which means slightly more difficult than Places and easier than Plantae. In addition, few-shot difficulty of tieredImageNet-test is 0.414, which means more difficult than EuroSAT and easier than Places.

Table 15 describes the few-shot performance under the same domain; miniImageNet → miniImageNet-test and tieredImageNet → tieredImageNet-test. As expected, they have large similarity and high difficulty. Therefore, (1) SL is more powerful than SSL, (2) MSL is a better strategy than both SL and SSL, and (3) two-stage pre-training boosts performance.

Table 15. 5way- k shot FSL performance of the models pre-trained: miniImageNet → miniImageNet-test and tieredImageNet → tieredImageNet-test. We report the average accuracy and its 95% confidence interval over 600 few-shot episodes. B and S indicate base and strong augmentations, respectively. For MSL and SL→MSL, γ is set to 0.875.

Pre-train Scheme	Method	Aug.	miniImageNet		tieredImageNet	
			$k=1$	$k=5$	$k=1$	$k=5$
SL	Default	B	54.89±.80	77.92±.59	60.98±.92	78.88±.68
		S	57.30±.81	77.32±.65	60.77±.92	78.36±.71
SSL	SimCLR	B	42.69±.88	60.42±.81	51.63±.93	67.62±.84
		S	54.39±.92	71.62±.79	66.67±1.02	80.60±.75
	BYOL	B	39.32±.76	58.36±.80	48.11±.88	69.72±.80
		S	44.71±.80	63.66±.77	59.00±.97	78.59±.70
MSL	SimCLR	S	63.15±.85	80.03±.63	74.24±.94	86.90±.64
	BYOL	S	58.59±.84	78.17±.65	75.25±.92	88.37±.58
SL→SSL	SimCLR	S	65.48±.89	83.84±.59	68.27±1.04	81.22±.75
	BYOL	S	55.76±.83	78.43±.61	65.78±.99	80.93±.66
SL→MSL	SimCLR	S	67.24±.86	85.02±.52	74.14±.96	87.38±.62
	BYOL	S	61.10±.82	82.35±.58	75.47±.90	88.72±.58